Mutiferroicity in Spin Ice: Bilayered crystal of Magnetic Monopoles

Arsen GUKASOV

Laboratoire Léon Brillouin,CEA-CNRS, Saclay, France

Double layered monopole structure in spin liquide

A Sazonov, A Gukasov, I Mirebeau and P Bonville.

***Phys. Rev. B* 85**, 214420 (2012)

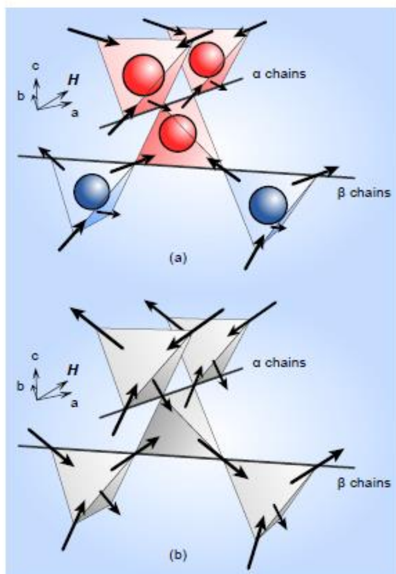

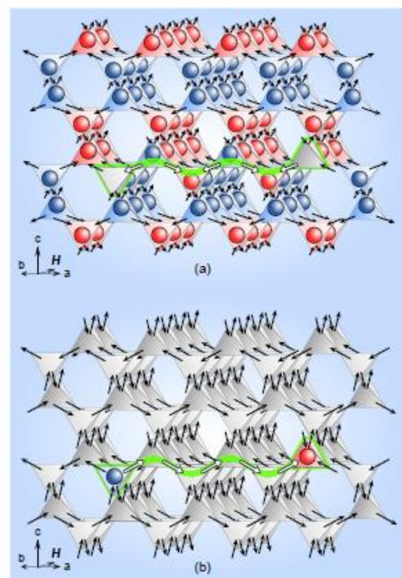

FIG. 3. Magnetic structures of $Tb_2Ti_2O_7$ spin liquid and $Ho_2Ti_2O_7$ spin ice in a [110] field. (a) Antimonopolar (double-layered monopolar) structure of $Tb_2Ti_2O_7$. (b) Magnetically vacuum state of $Ho_2Ti_2O_7$.

FIG. 4. Elementary excitations in $Tb_2Ti_2O_7$ spin liquid and $Ho_2Ti_2O_7$ spin ice. (a) Antimonopolar (double-layered monopolar) structure of $Tb_2Ti_2O_7$ with vacuum pair excitations. (b) Magnetically vacuum state of $Ho_2Ti_2O_7$ with

PHYSICAL REVIEW B **91**, 214422 (2015)

Multiferroicity in spin ice: Towards magnetic crystallography of $Tb_2Ti_2O_7$ in a field

L. D. C. Jaubert[1] and R. Moessner[2]
[1] *Okinawa Institute of Science and Technology Graduate University, Onna-son, Okinawa 904-0495, Japan*
[2] *Max-Planck-Institut für Physik komplexer Systeme, 01187 Dresden, Germany*
(Received 10 February 2015; revised manuscript received 22 May 2015; published 17 June 2015)

We combine two aspects of magnetic frustration, multiferroicity and emergent quasiparticles in spin liquids, by studying magnetoelectric monopoles. Spin ice offers to couple these emergent topological defects to external fields, and to each other, in unusual ways, making it possible to lift the degeneracy underpinning the spin liquid and to potentially stabilize novel forms of charge crystals, opening the path to a "magnetic crystallography." In developing the general phase diagram including nearest-neighbor coupling, Zeeman energy, and electric and magnetic dipolar interactions, we uncover the emergence of a bilayered crystal of *singly charged* monopoles, whose stability, remarkably, is strengthened by an external [110] magnetic field. Our theory is able to account for the ordering process of $Tb_2Ti_2O_7$ in a large field for reasonably small electric energy scales.

DOI: 10.1103/PhysRevB.91.214422 PACS number(s): 75.10.Jm, 71.27.+a, 75.85.+t

frustration, multiferroicity, emergent quasiparticles, spin liquids, magnetoelectric monopoles, topological defects

In spin ice materials, frustration takes place on the pyrochlore lattice and the so-called ice rules which require two spins to point inward and two outward for each tetrahedron.
These constraints support an extensively degenerate ground state and ensure the local conservation of magnetic fluxes described as a coarse-grained divergence-free condition, categorizing the spin ice ground state as a Coulomb spin liquid by analogy with Maxwell's electromagnetism, where excitations take the form of classical magnetic monopoles.

2012 CMD Europhysics Prize Winners

Steven Bramwell, Claudio Castelnovo, Santiago Grigera, Roderich Moessner, Shivaji Sondhi and Alan Tennant

"for the prediction and experimental observation of magnetic monopoles in spin ice"

Ivan Ryzhkin

ISSP
Condensed Matter Physics
Verified email at issp.ac.ru

Title 1–20	Cited by	Year
Conductivity of quasi-one-dimensional metal systems AA Abrikosov, IA Ryzhkin Advances in Physics 27 (2), 147-230	283	1978
Magnetic relaxation in rare-earth oxide pyrochlores IA Ryzhkin Journal of Experimental and Theoretical Physics 101 (3), 481-486	148	2005
Physical mechanisms responsible for ice adhesion IA Ryzhkin, VF Petrenko The Journal of Physical Chemistry B 101 (32), 6267-6270	75	1997
Surface states of charge carriers and electrical properties of the surface layer of ice VF Petrenko, IA Ryzhkin The Journal of Physical Chemistry B 101 (32), 6285-6289	38	1997
Violation of ice rules near the surface: A theory for the quasiliquid layer IA Ryzhkin, VF Petrenko Physical review B 65 (1), 012205	26	2001
The configurational entropy in the Jaccard theory of the electrical properties of ice IA Ryzhkin, RW Whitworth Journal of Physics: Condensed Matter 9 (2), 395	26	1997

Citation indices	All	Since 2012
Citations	859	342
h-index	12	8
i10-index	15	8

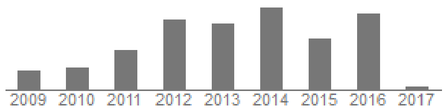

Co-authors View all...

Иван Цыбулин

OUTLINE

- Magnetic Monopoles and Dirac Strings
- Frustrated Magnets and Spin Ice state
- Emergent “Magnetic Monopoles”
- Bilayered crystal of “Magnetic Monopoles”

Electricity

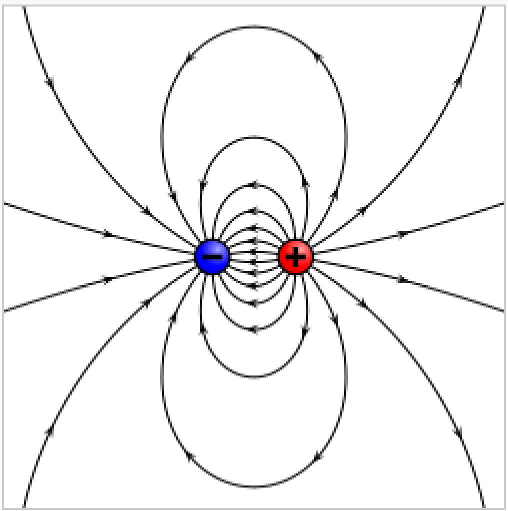

Electric field lines of two opposing charges separated by a finite distance.

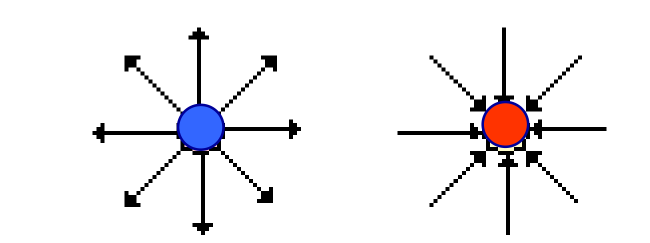

Polar molecules (electric dipoles)

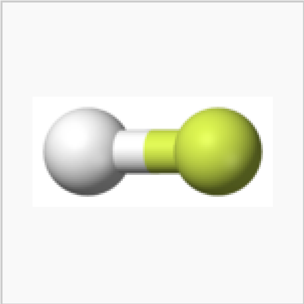

Hydrogen fluoride: the more electronegative fluoride atom is shown in yellow

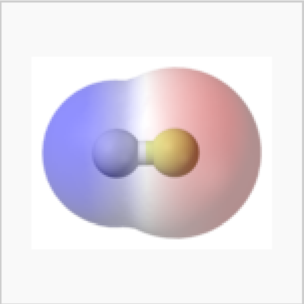

Hydrogen fluoride: red represents partially negatively charged regions

Magnetism

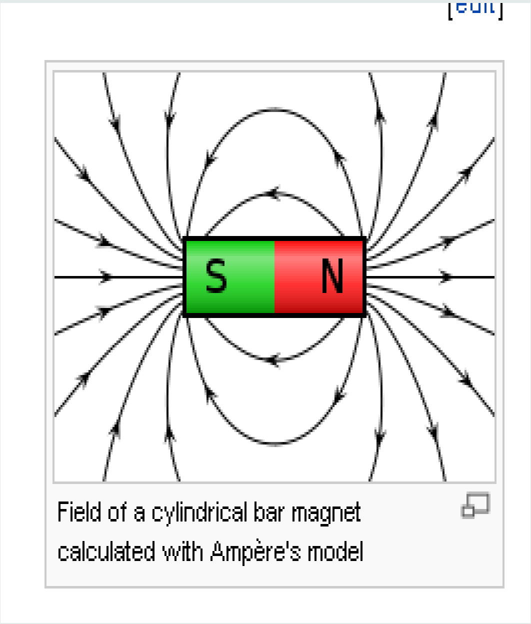

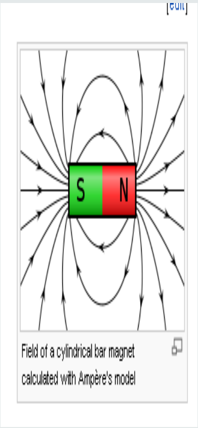

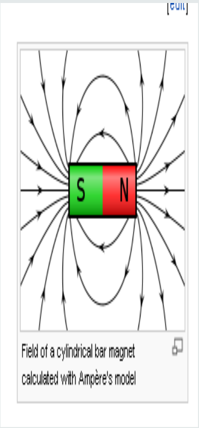

Pierre Curie in 1894 proposed magnetic monopoles

Electricity "true" dipoles
Magnetism "point" dipole

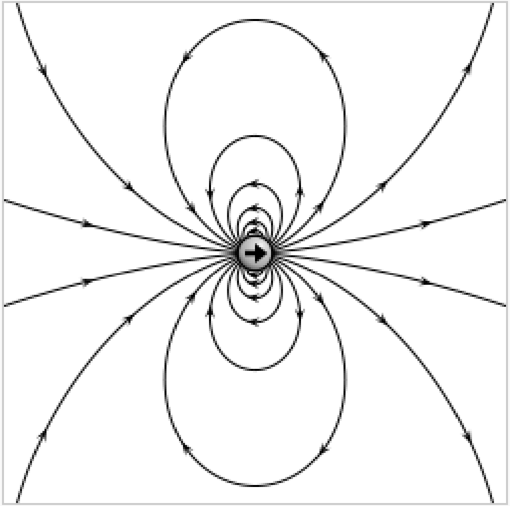

Field lines of a point dipole of any type, electric, magnetic, acoustic, ...

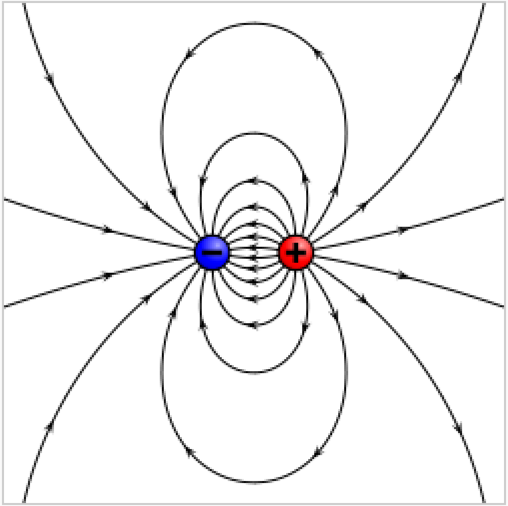

Electric field lines of two opposing charges separated by a finite distance.

Electro- and Magneto-statics

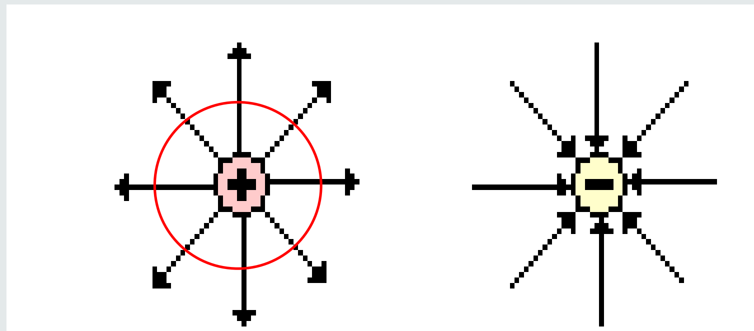

Gauss's law:	$\nabla \cdot \mathbf{E} = 4\pi\rho_e$
Gauss's law for magnetism:	$\nabla \cdot \mathbf{B} = 0$

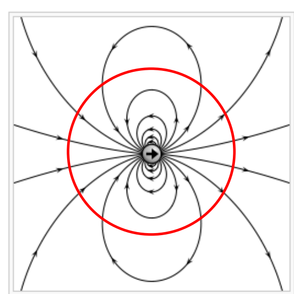

Field lines of a point dipole of any type, electric, magnetic, acoustic, ...

Divergence free field

Fields

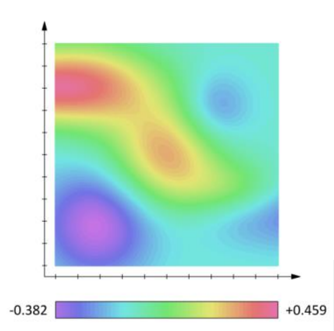

Scalar Field associates a scalar value in a subset of space:
Temperature, Pressure, Charge etc.
In common life : Oil fields, Gaz fields, Corn fields

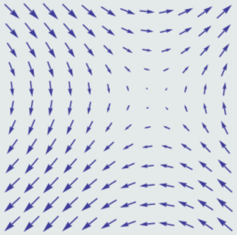

Vector Field associates a vector value in a subset of space:
Electric, Magnetic, gravitation, stress etc.
In common life : wind, traffic, rivers, pipes

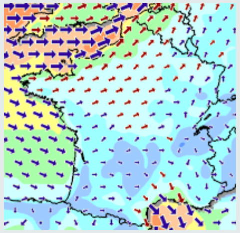

Vector Fields

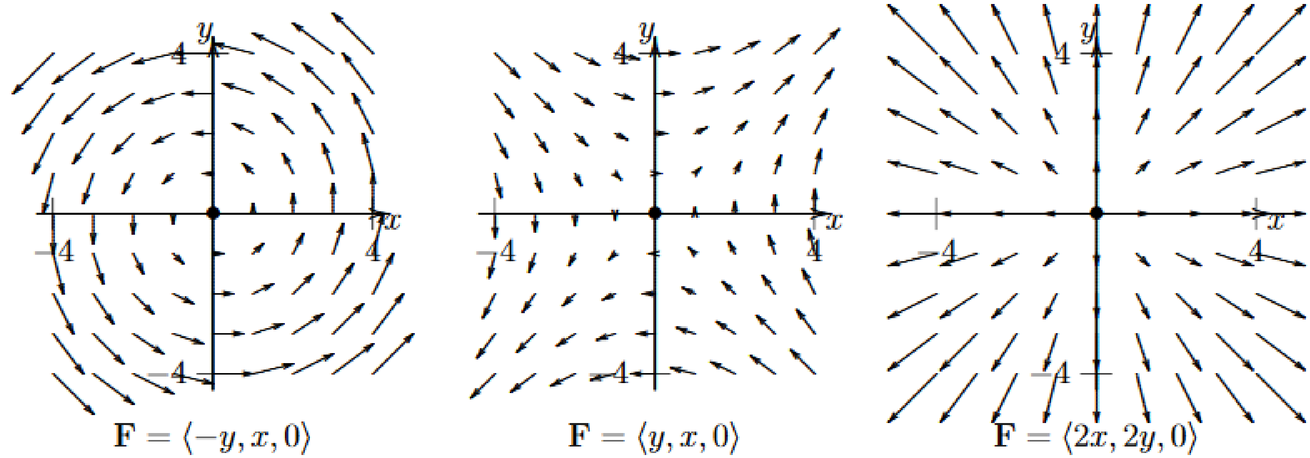

(a) $\operatorname{div} \mathbf{F} = 0$
$\operatorname{curl} \mathbf{F} = \langle 0, 0, 2 \rangle$

(b) $\operatorname{div} \mathbf{F} = 0$
$\operatorname{curl} \mathbf{F} = \mathbf{0}$

(c) $\operatorname{div} \mathbf{F} = 4$
$\operatorname{curl} \mathbf{F} = \mathbf{0}$

Maxwell Electrodynamics

Name	Without magnetic monopoles
Gauss's law:	$\nabla \cdot \mathbf{E} = 4\pi \rho_e$
Gauss's law for magnetism:	$\nabla \cdot \mathbf{B} = 0$
Maxwell–Faraday equation (Faraday's law of induction):	$-\nabla \times \mathbf{E} = \frac{1}{c}\frac{\partial \mathbf{B}}{\partial t}$
Ampère's law (with Maxwell's extension):	$\nabla \times \mathbf{B} = \frac{1}{c}\frac{\partial \mathbf{E}}{\partial t} + \frac{4\pi}{c}\mathbf{j}_e$

Quantised Singularities in the Electromagnetic Field.

By P. A. M. Dirac, F.R.S., St. John's College, Cambridge.

(Received May 29, 1931.)

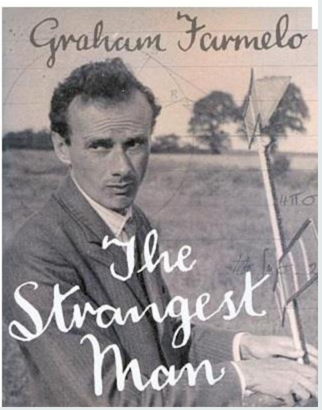

http://rspa.royalsocietypublishing.org/content/133/821/60.full.pdf

Dirac 1931: *"The most powerful method of advance that can be suggested at present is to employ all the resources of pure mathematics in attempts to perfect and generalise the mathematical formalism" .*

Name	Without magnetic monopoles	With magnetic monopoles (hypothetical)
Gauss's law:	$\nabla \cdot \mathbf{E} = 4\pi \rho_\mathrm{e}$	$\nabla \cdot \mathbf{E} = 4\pi \rho_\mathrm{e}$
Gauss's law for magnetism:	$\nabla \cdot \mathbf{B} = 0$	$\nabla \cdot \mathbf{B} = 4\pi \rho_\mathrm{m}$
Maxwell–Faraday equation (Faraday's law of induction):	$-\nabla \times \mathbf{E} = \frac{1}{c}\frac{\partial \mathbf{B}}{\partial t}$	$-\nabla \times \mathbf{E} = \frac{1}{c}\frac{\partial \mathbf{B}}{\partial t} + \frac{4\pi}{c}\mathbf{j}_\mathrm{m}$
Ampère's law (with Maxwell's extension):	$\nabla \times \mathbf{B} = \frac{1}{c}\frac{\partial \mathbf{E}}{\partial t} + \frac{4\pi}{c}\mathbf{j}_\mathrm{e}$	$\nabla \times \mathbf{B} = \frac{1}{c}\frac{\partial \mathbf{E}}{\partial t} + \frac{4\pi}{c}\mathbf{j}_\mathrm{e}$

"This result is too beautiful to be false. It is more important to have beauty in one's equation than to have them fit experiment." P aul Dirac

P.A.M. Dirac, Proc. Roy. Soc. A 133, 60 1931

The theoretical reciprocity between electricity and magnetism is perfect. Instead of discussing the motion of an electron in the field of a fixed magnetic pole, as we did in § 4, we could equally well consider the motion of a pole in the field of fixed charge. This would require the introduction of the electromagnetic potentials B satisfying

$$\mathbf{E} = \text{curl } \mathbf{B}, \qquad \mathbf{H} = \frac{1}{c}\frac{\partial \mathbf{B}}{\partial t} + \text{grad } \mathbf{B}_0,$$

to be used instead of the A's in equations (6). The theory would now run quite parallel and would lead to the same condition (9) connecting the smallest pole with the smallest charge.

There remains to be discussed the question of why isolated magnetic poles are not observed. The experimental result (1) shows that there must be some cause of dissimilarity between electricity and magnetism (possible connected with the cause of dissimilarity between electrons and protons) as the result of which we have, not $\mu_0 = e$, but $\mu_0 = 137/2 \cdot e$. This means that the attractive force between two one–quantum poles of opposite sign is $(137/2)^2 = 4692\frac{1}{4}$ times that between electron and proton. This very large force may perhaps account for why poles of opposite sign have never yet been separated.

Under these circumstances one would be surprised if Nature had made no use of it.

Search for Monopole

Passing trough a Solenoid of 1 meter with H= 250 Gs
Monopole gain energy 500 Mev

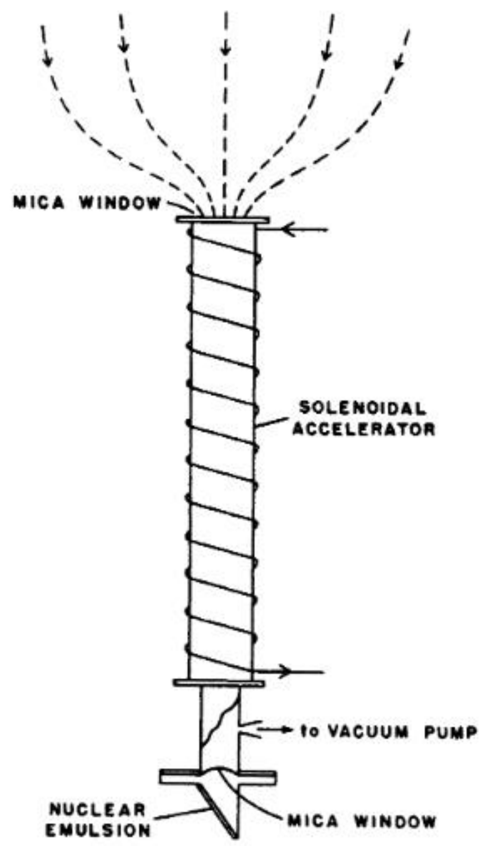

FIG. 1. Schematic diagram of an instrument to detect magnetic monopoles arriving at the earth's surface.

VOLUME 48, NUMBER 20 PHYSICAL REVIEW LETTERS 17 MAY 1982

First Results from a Superconductive Detector for Moving Magnetic Monopoles

Blas Cabrera
Physics Department, Stanford University, Stanford, California 94305
(Received 5 April 1982)

A velocity- and mass-independent search for moving magnetic monopoles is being performed by continuously monitoring the current in a 20-cm^2-area superconducting loop. A single candidate event, consistent with one Dirac unit of magnetic charge, has been detected during five runs totaling 151 days. These data set an upper limit of 6.1×10^{-10} cm^{-2} sec^{-1} sr^{-1} for magnetically charged particles moving through the earth's surface.

PACS numbers: 14.80.Hv

VOLUME 48, NUMBER 20 PHYSICAL REV

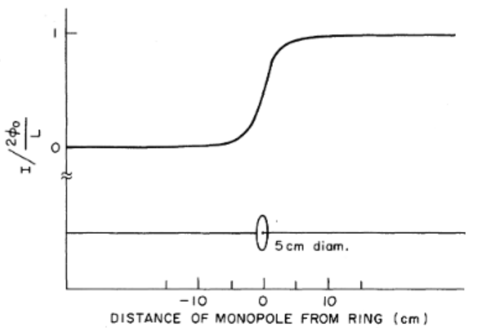

FIG. 1. Induced current in a superconducting ring for an axial monopole trajectory.

VOLUME 48, NUMBER 20 PHYSICAL REVIEW LETTERS 17 MAY 1982

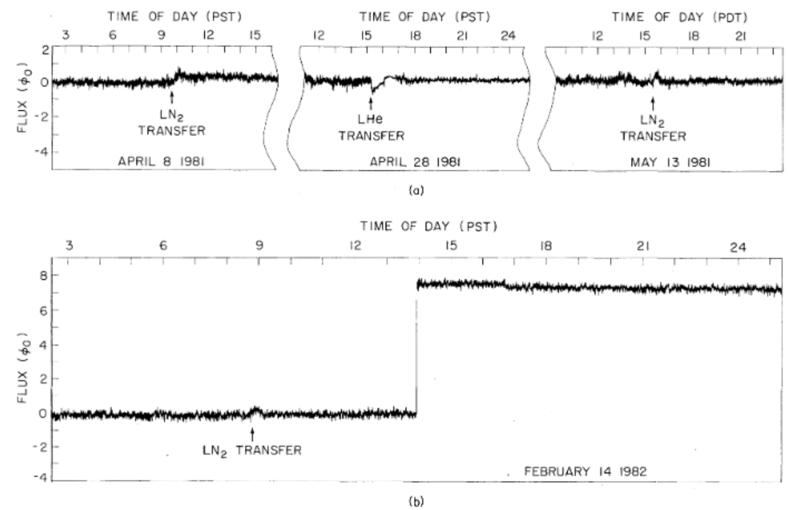

FIG. 2. Data records showing (a) typical stability and (b) the candidate monopole event.

Grand Unified Theory (Théorie du Tout)

Interaction	Théorie courante	Médiateurs	Masse (GeV/c^2)	Puissance relative approximative	Rayon d'action (m)	Dépendance de distance
Forte	Chromodynamique quantique (QCD)	8 gluons	0	1	$2{,}5 \cdot 10^{-15}$	$\frac{1}{r^7}$
Électromagnétique	Électrodynamique quantique (QED)	photon	0	10^{-2}	∞	$\frac{1}{r^2}$
Faible	Théorie électrofaible	W^+, W^-, Z^0	80, 80, 91	10^{-13}	10^{-18}	$\frac{1}{r^5}$ à $\frac{1}{r^7}$
Gravitation	Relativité générale	graviton (postulé)	0	10^{-38}	∞	$\frac{1}{r^2}$

es [modifier]

Magnetic monopole

In 1974 G. 't Hooft and independently A. M. Polyakov showed that magnetically charged particles are necessarily present in all true unification theories.

These theories predict the same long-range field and thus the same charge g_0 as the Dirac solution; now, however, the near field is also specified, leading to a calculable mass.

$$M \approx 10^{19}\,\mathrm{GeV}\ (!) \approx 10^{32}\,\mathrm{K} \approx 0.2\ \mathrm{mg}\ (!)$$

Lorentz medal

Les lauréats [modifier | modifier le code]

- 1927 : Max Planck, Allemagne
- 1931 : Wolfgang Ernst Pauli, Suisse
- 1935 : Peter Debye, Allemagne
- 1939 : Arnold Sommerfeld, Allemagne
- 1947 : Hendrik Anthony Kramers, Pays-Bas
- 1953 : Fritz London, États-Unis
- 1958 : L. Onsager, États-Unis
- 1962 : Rudolf Ernst Peierls, Grande-Bretagne
- 1966 : F.J. Dyson, États-Unis
- 1970 : G.E. Uhlenbeck, États-Unis
- 1974 : John Hasbrouck van Vleck, États-Unis
- 1978 : Nicolaas Bloembergen, États-Unis
- 1982 : Anatole Abragam, France
- 1986 : Gerard 't Hooft, Pays-Bas
- 1990 : P.-G. de Gennes, France
- 1994 : A.M. Polyakov, États-Unis
- 1998 : Carl Edwin Wieman et Eric Allin Cornell, États-Unis
- 2002 : Frank Wilczek, États-Unis
- 2006 : L.P. Kadanoff, États-Unis
- 2010 : Edward Witten, États-Unis
- 2014 : Michael Berry, Royaume-Uni

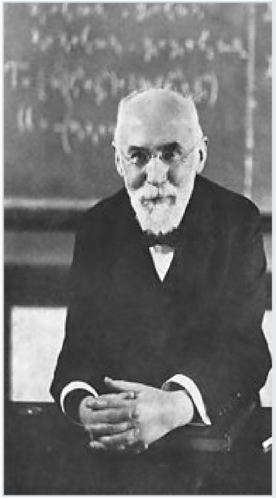

H. A. Lorentz.

Notes et références [modifier | modifier le code]

Dirac string

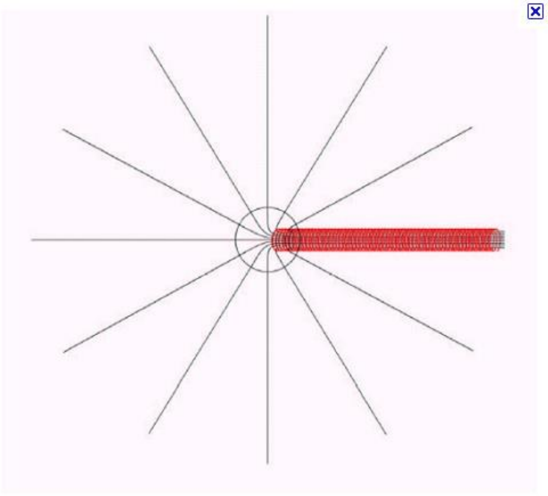

Figure 2: The vector potential of a monopole is singular on a string. When the string carries an integer number of flux quanta it can be gauged away.

Videos illustrating why Dirac's strings do not obstruct electrons trajectories:

http://www.youtube.com/watch?v=CYBqIRM8GiY

http://www.youtube.com/watch?v=EgAK9JDZ-q4

What's the Dirac string?

Dirac pointed out that the magnetic field generated by a magnetic monopole would be undistinguishable by the one generated by an infinitely thin solenoid (now called Dirac string) running from the monopole to another monopole of opposing charge (or to infinity !).

Spin Ice and Frustrated magnets

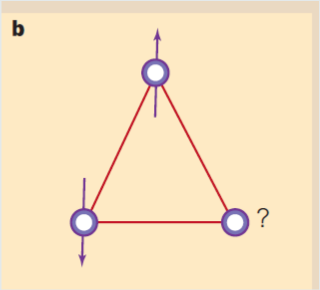

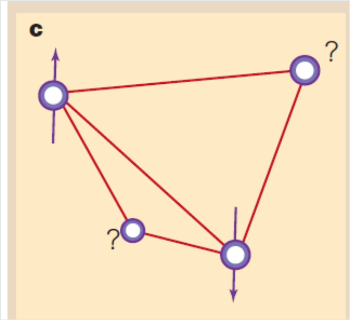

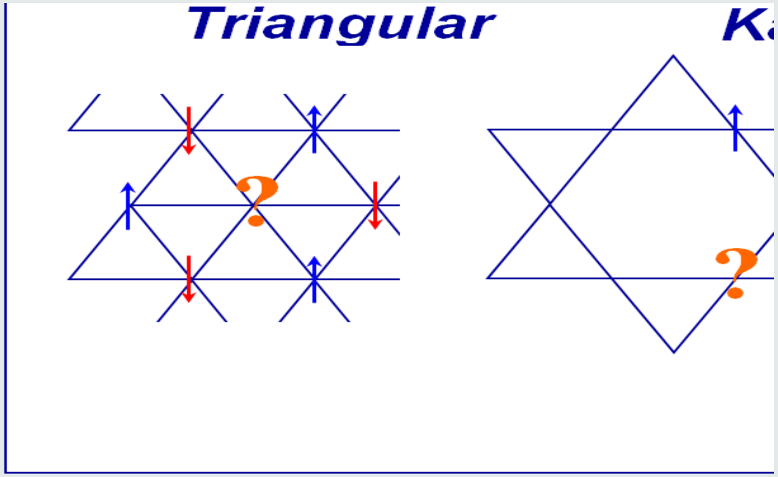

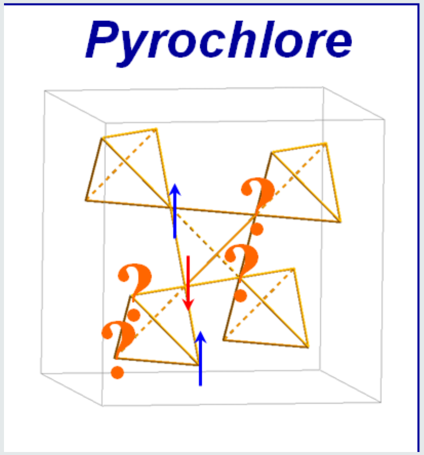

Definition***: Frustration arises when it is impossible to satisfy all interactions on the lattice at the same time.***

Pyrochlores;Symmetry of R Site in $R_2T_2O_7$

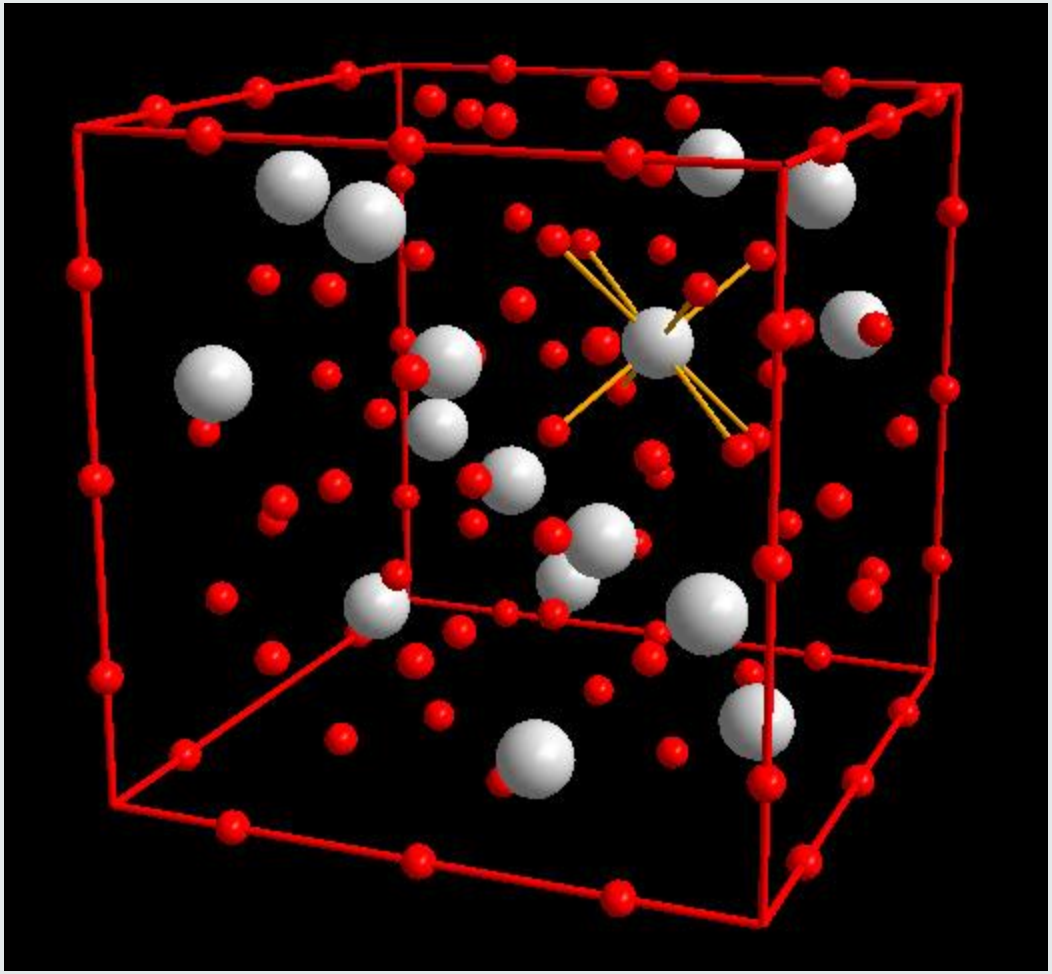

2x Tb-O1 2.19 A

6 xTb-O2 2.51 A

Pyrochlore compounds $R_2T_2O_7$

R^{3+} rare earth ion on tetrahedra lattice

T nonmagnetic 3d ion

Fd-3m

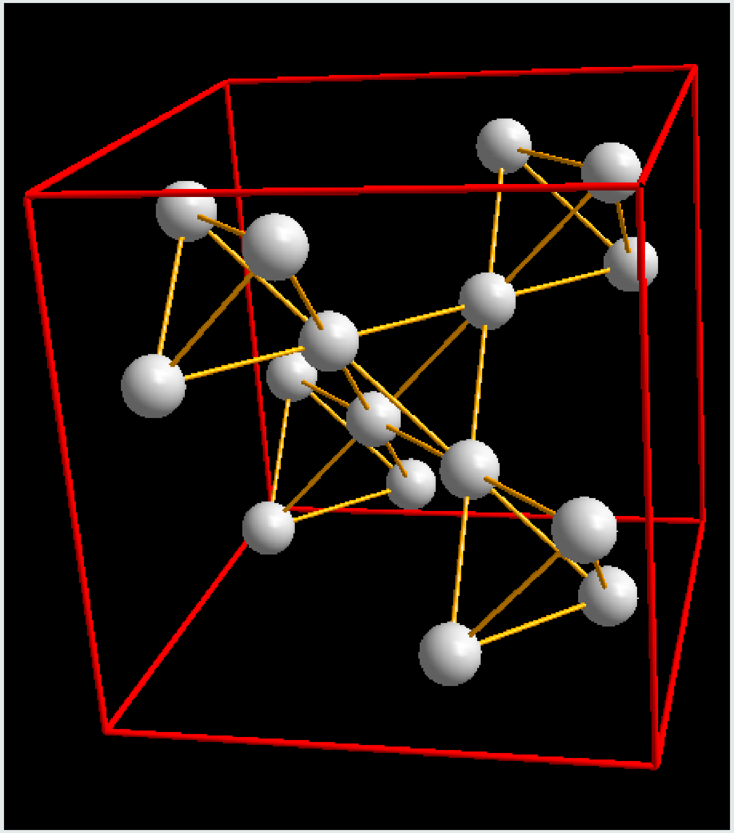

Spin Ice $Dy_2Ti_2O_7$

M.Harris, S Bramwell. Nature **399** (1999) 311 & A.P.Ramirez *et al*, Nature **399** (1999) 333

- Residual low-T entropy: Pauling entropy for water ice $S_0 = (1/2)\ln(3/2)$ Ramirez *et al.*:

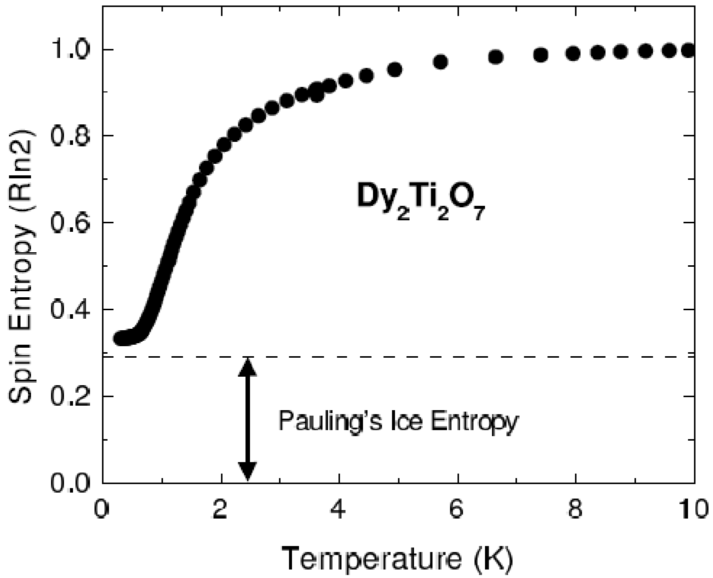

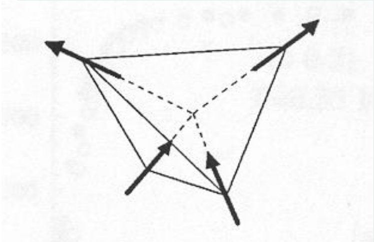

- Pauling estimate: ground-state constraints independent

$$N_{gs} = 2^n (6/16)^{n/2} = (3/2)^{n/2} \Rightarrow S_0 = \frac{1}{2}\ln\frac{3}{2}$$

Cooling of Spin ice in field takes longer than without it

Residual entropy of Ice.
Pauling entropy

[Contribution from the Chemical Laboratory of the University of California]

The Entropy of Water and the Third Law of Thermodynamics. The Heat Capacity of Ice from 15 to 273°K.

By W. F. Giauque and J. W. Stout

made by Rossini[2] and various equilibrium data, including those relating to the reactions[3]

$$HgO + H_2 = Hg + H_2O$$
$$Hg + {}^1/_2O_2 = HgO$$

indicated that the $\int_0^T C_p \mathrm{d} \ln T$ for water did not give the correct entropy. That this was so became a certainty when Giauque and Ashley[4] calculated the entropy of gaseous water from its band spectrum and showed that an entropy discrepancy of about one calorie per degree per mole existed. They presumed this to be due to false equilibrium in ice at low temperatures.

Water is a substance of such importance that we considered further experimental investigation to be desirable not only to check the above discrepancy but especially to see whether slow cooling or other conditions favorable to the attainment of equilibrium could alter the experimental result.

Apparatus.—In order to prevent strains in the resistance thermometer when the water was frozen a double-walled calorimeter, Fig. 1, was constructed. The outside wall was of copper, 0.5 mm. thick, 4.4 cm. o. d., and 9 cm. long. The inside copper wall, 0.5 mm. thick, was tapered, being 3.8 cm. o. d. at the bottom and 4.0 cm. o. d. at the upper end. The top of the inner container was made from a thin copper sheet, 0.2 mm. thick, which prevented the transmission of strains to the resistance thermometer. The neck for filling the calorimeter was in the center of this sheet. A series of thin circular slotted vanes of copper were soldered to the inner container, and the assembly forced inside the outer tube. A heavy copper plate, 1 mm. thick inside the inner wall, and 2 mm. thick between the walls, served as the bottom of both tubes. The thermocouple was soldered into tube D by means of Rose's metal.

the basis of these comparisons a small correction to the original calibration was readily made.

Helium gas was introduced into the space between the two walls by means of a German silver tube, A. A similar German silver tube was soldered by means of Wood's metal into the cap, B. The sample, C, was transferred through this tube into the calorimeter, and helium gas at one atmosphere pressure admitted. The German silver tube was then heated and removed from the cap, leaving the hole sealed with Wood's metal. After the measurements on the full calorimeter had been completed, the calorimeter was heated to the melting point of the Wood's metal (72°C.) and the water completely pumped out without dismantling the apparatus. The heat capacity of the empty calorimeter was then measured.

The remainder of the heat capacity apparatus, the method of making the measurements and calculations, and accuracy considerations were similar to those previously described.[1a,c]

Purification of Water.—Distilled water from the laboratory still was transferred into the vacuum-tight purification apparatus constructed from Pyrex glass. The apparatus was evacuated to remove dissolved gases, and flushed out several times with helium gas. The water was distilled into a receiving bulb, the first fraction being discarded. The calorimeter had previously been attached to the purification system and evacuated. When sufficient water had

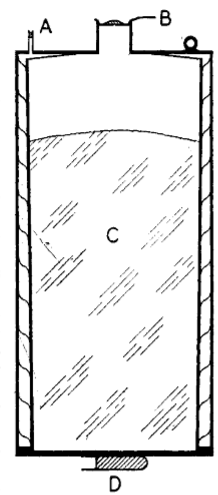

Third law of thermodynamics requires all substances to have zero entropy (S=0) at *T = 0 K.*

Bernal-Fowler rules and Pauling Entropy

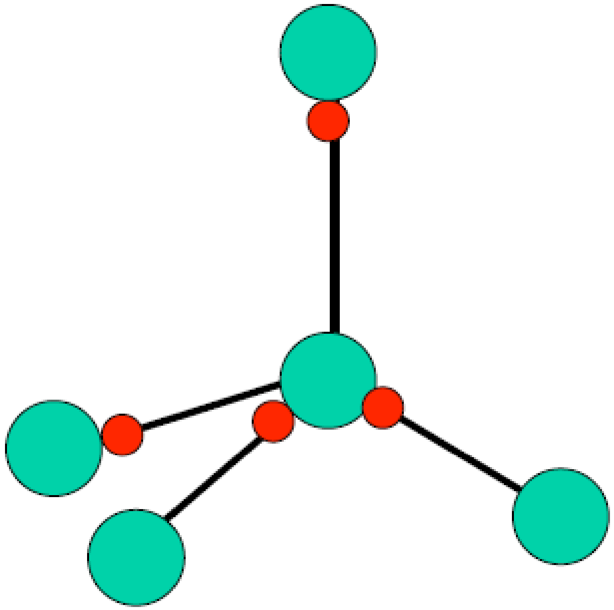

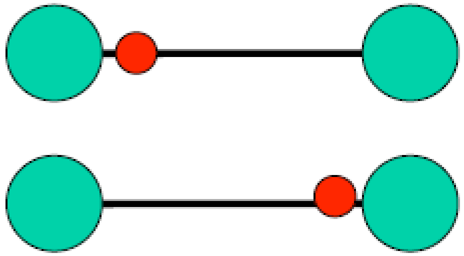

Each Hydrogen takes 2 positions.
For 1 mole of H_20

$$\Omega^0 = 2^{2N}$$

$2^4=16$ configs for each O^{2-}, 6/16 satisfy Bernal Fowler rules:

$$\Omega \approx 2^{2N}\left(\frac{3}{8}\right)^N = \left(\frac{3}{2}\right)^N$$ => $$S \approx R \log\left(\frac{3}{2}\right)$$ Per mole

Water Ice and Spin Ice

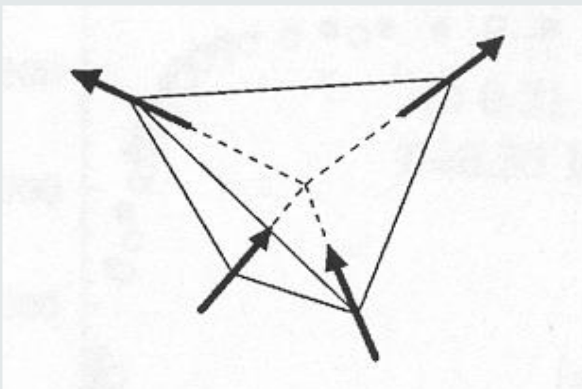

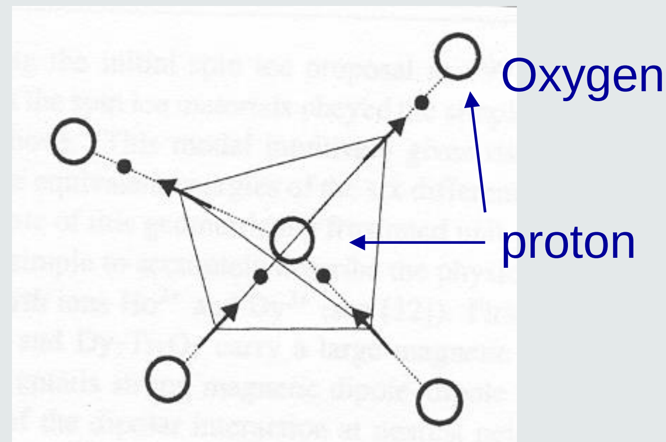

If ferromagnetic interactions, the ground configuration is « two in – two out » spins

$\Longrightarrow$

Similar to ice ground state: « two close – two far » protons with zero point entropy

Ice Rules in a tetrahedra

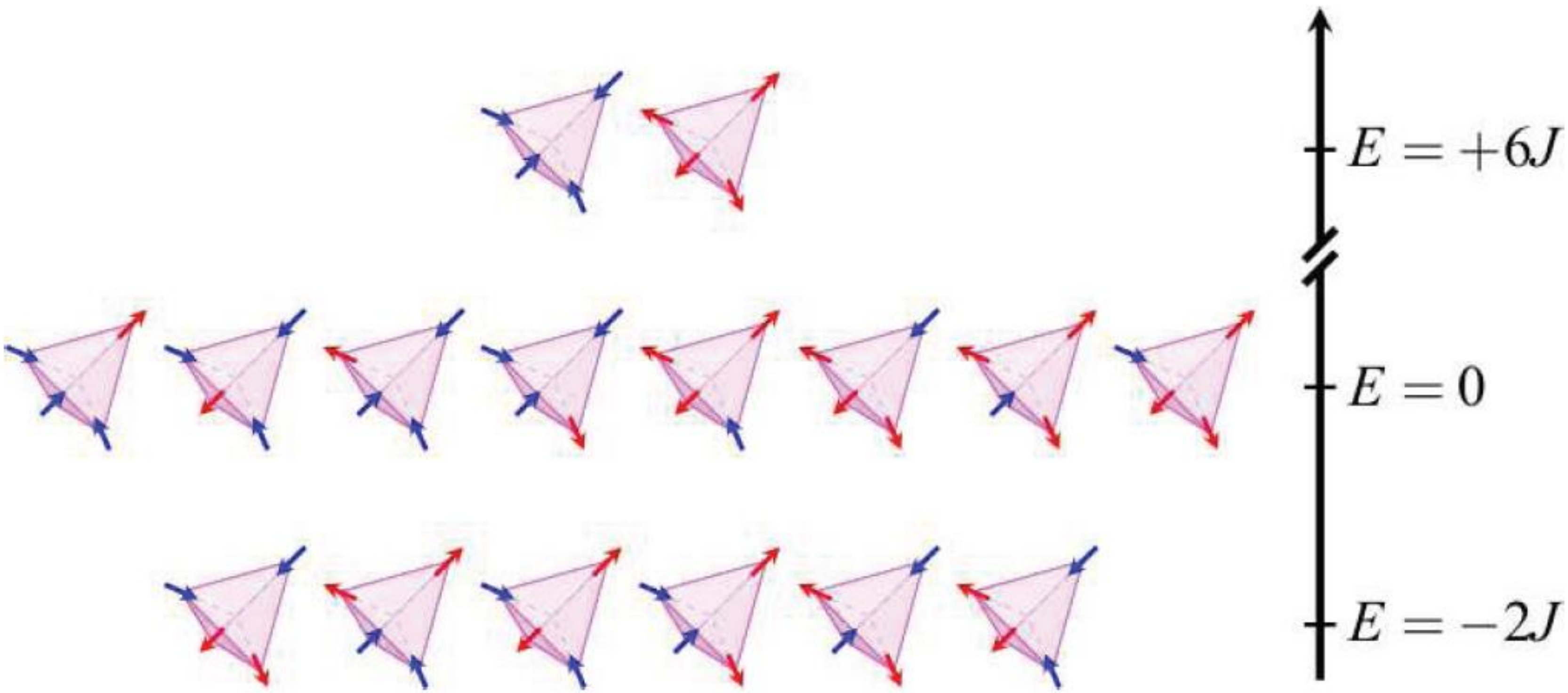

- Pauling estimate: ground-state constraints independent

$$N_{gs} = 2^n (6/16)^{n/2} = (3/2)^{n/2} \Rightarrow S_0 = \frac{1}{2} \ln \frac{3}{2}$$

Sip Ice as a Coulomb phase

Review: Christopher L. Henley. The Coulomb phase" in frustrated systems

The ice rules impose local constraints

Two spins in two spins out
=> A divergence free field

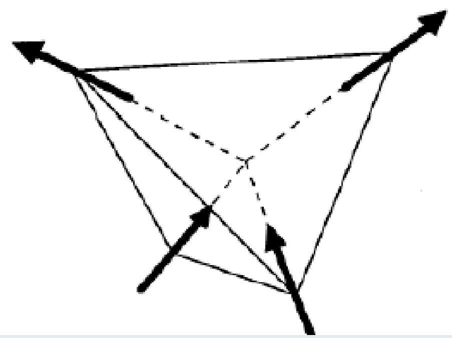

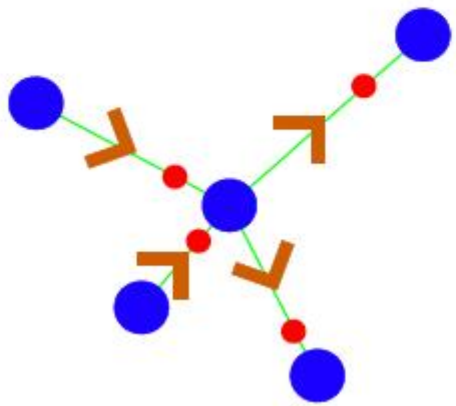

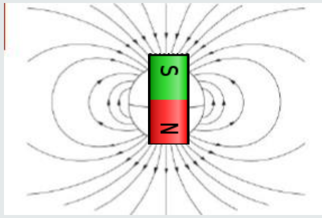

$$\vec{\nabla}.\vec{S}=0$$

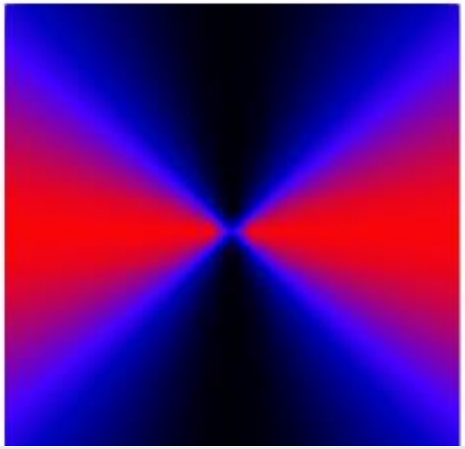

Gauss's law for magnetism:	$\nabla \cdot \mathbf{B} = 0$

Coarse Graining and LR correlations

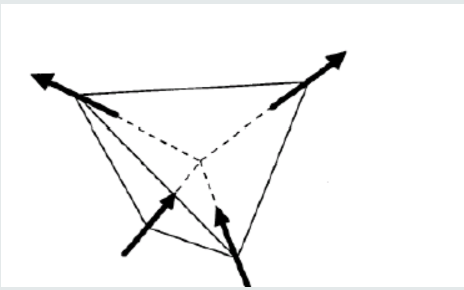

$$\vec{\nabla}.\vec{S}=0$$

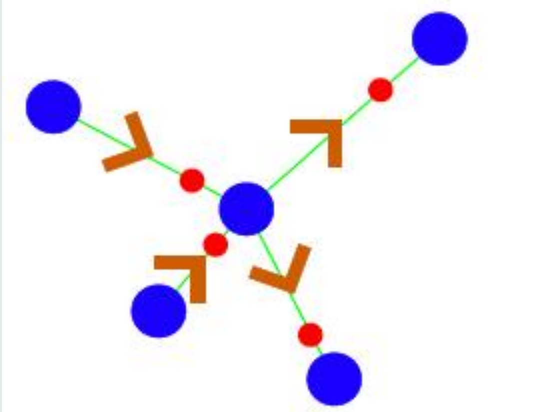

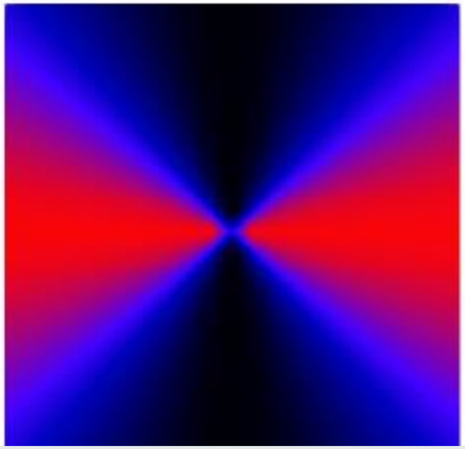

Pinch points in Coulomb phase

The ice rules impose local constraints

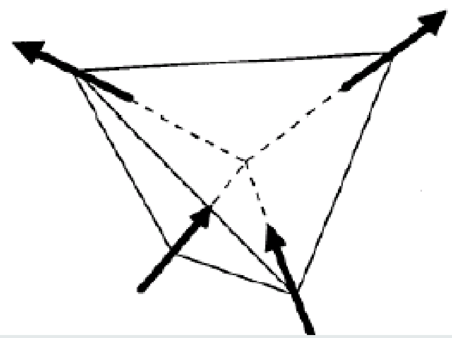

Two spins in two spins out
=> A divergence free field

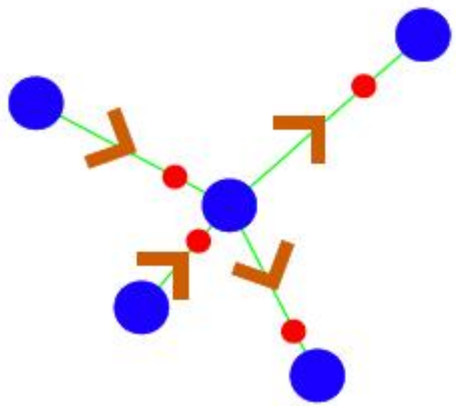

$$\vec{\nabla}.\vec{S}=0$$

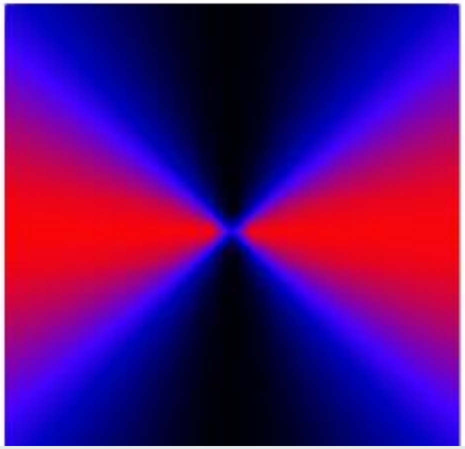

Pinch points in Coulomb phase

However, long range correlations do appear as « pinch » points in reciprocal space. (Youngblood and Axe, Phys. Rev. B 23, 232 (1981)).

Regions of intense diffuse scattering.

Narrowing=> correlations over large length scales

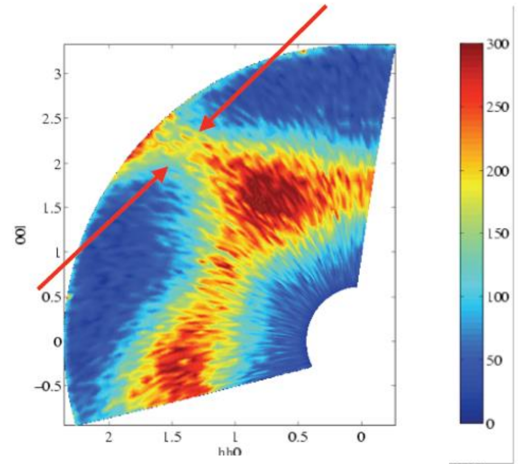

Single ... 2007)

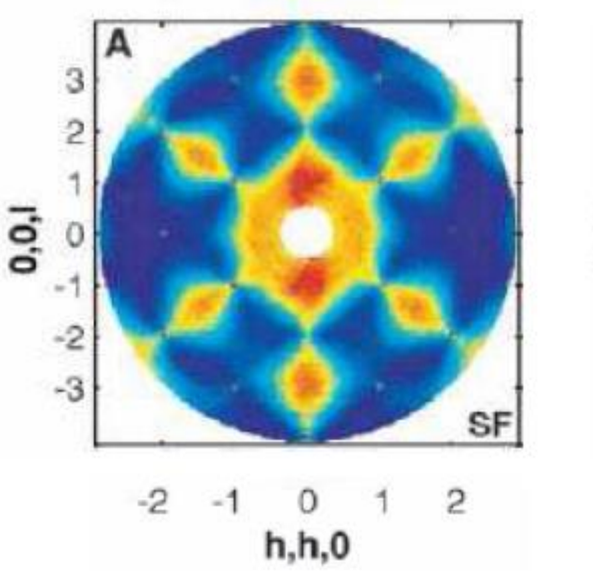

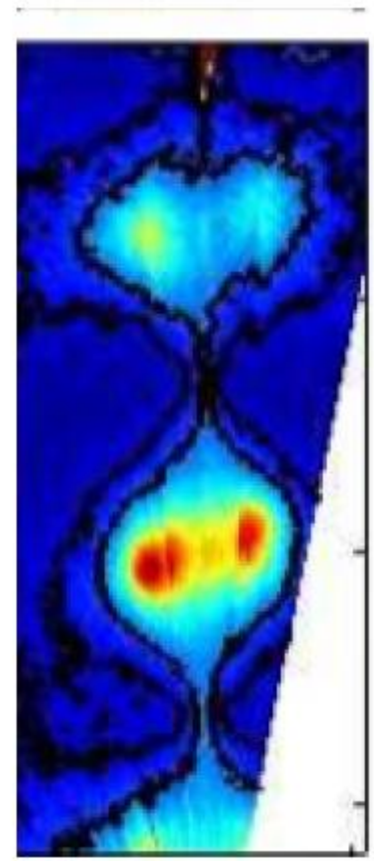

spin correlations in kagome ice
Fennell+Bramwell

6-vertex model

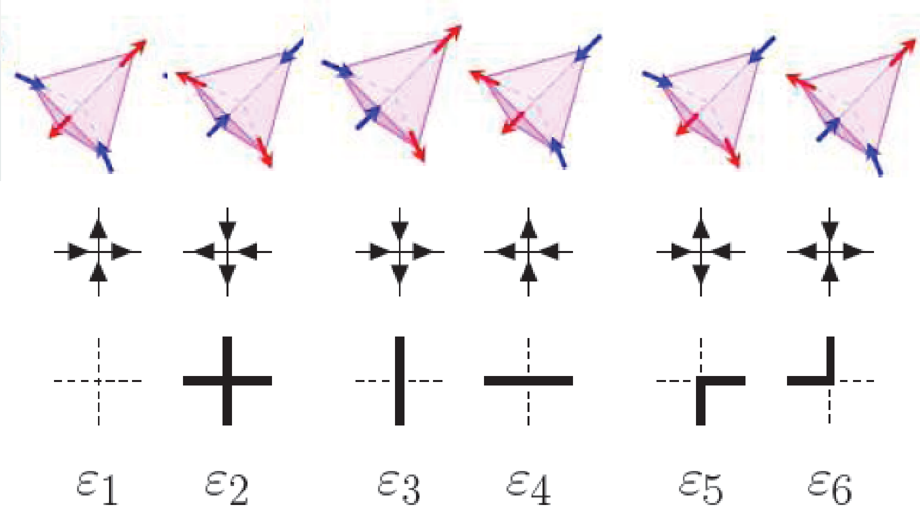

Figure II.9: **6-vertex model**: As for spin ice, each arrow can be seen as a dipole (either electric or magnetic). All 6 vertices respect the ice-rules and can be mapped onto a configuration of strings (second line). Each vertex has an energy ε_i that goes by pair (see equation (II.55).

lent under reversal of the arrows. This imposes certain conditions on the energies of the vertices.

$$\varepsilon_1 = \varepsilon_2, \quad \varepsilon_3 = \varepsilon_4, \quad \varepsilon_5 = \varepsilon_6 \tag{II.55}$$

Depending on the ratio of these energies, we can have very different behaviours:

- $\varepsilon_{i=1..6} = 0$: we recover Pauling's degeneracy of the *ice model*, solved by Lieb [Lie67d, Lie67c];
- $\varepsilon_{i=5,6} = 0$, $\varepsilon_{i=1..4} > 0$: this is the so-called F model proposed to describe antiferroelectrics because its ground state has a staggered polarisation;
- $\varepsilon_{i=1,2} = 0$, $\varepsilon_{i=3..6} > 0$: a given orientation of the polarisation is favoured (see left panel of figure II.10), characteristic of an ordered ferroelectric such as potassium

Топология

наука которая изучает свойства пространств, которые остаются неизменными при непрерывных деформациях.

наука которая может найти общее в том в чем нет ничего общего

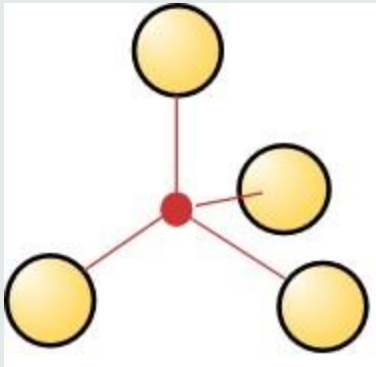

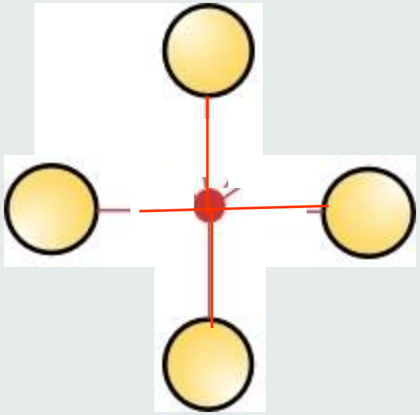

Топология

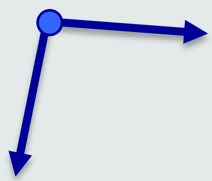

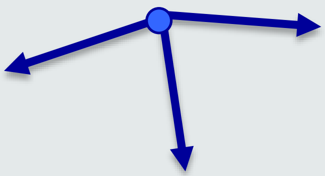

6-vertex model

- $\varepsilon_{i=1,2} = 0, \ \varepsilon_{i=3..6} > 0$: **FE**

- $\varepsilon_{i=1..6} = 0$: **spin-ice**

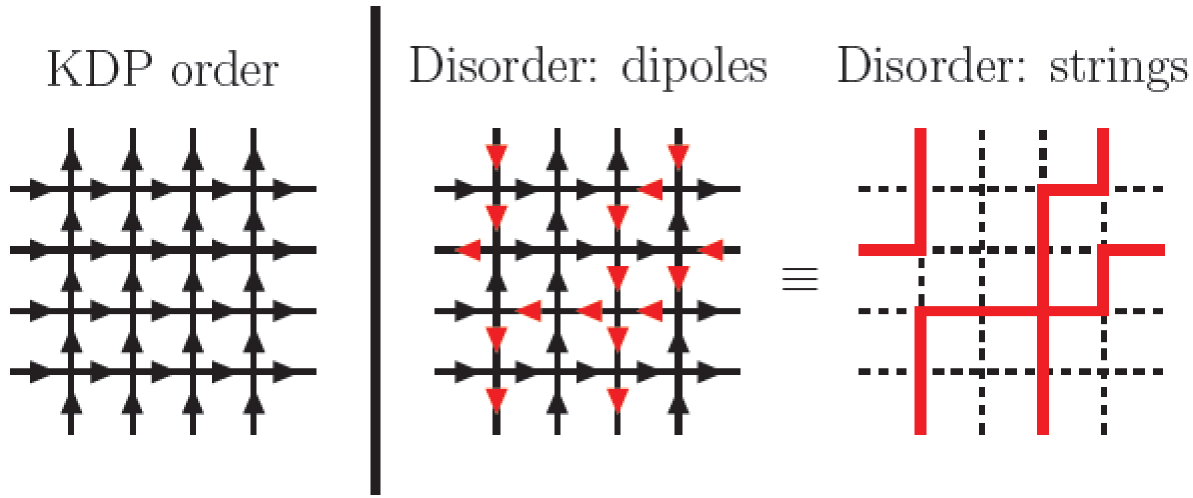

Figure II.10: **Configurations of the 6-vertex model:** *Left:* One of the two ground states of the KDP model with a net polarisation pointing north-east. *Right:* an example of disordered state represented with both dipoles and strings. We impose periodic boundary conditions.

6-vertex model

- $\varepsilon_{i=1,2} = 0,\ \varepsilon_{i=3..6} > 0$:

FE

$\varepsilon_{i=1..6} = 0$:

spin-ice

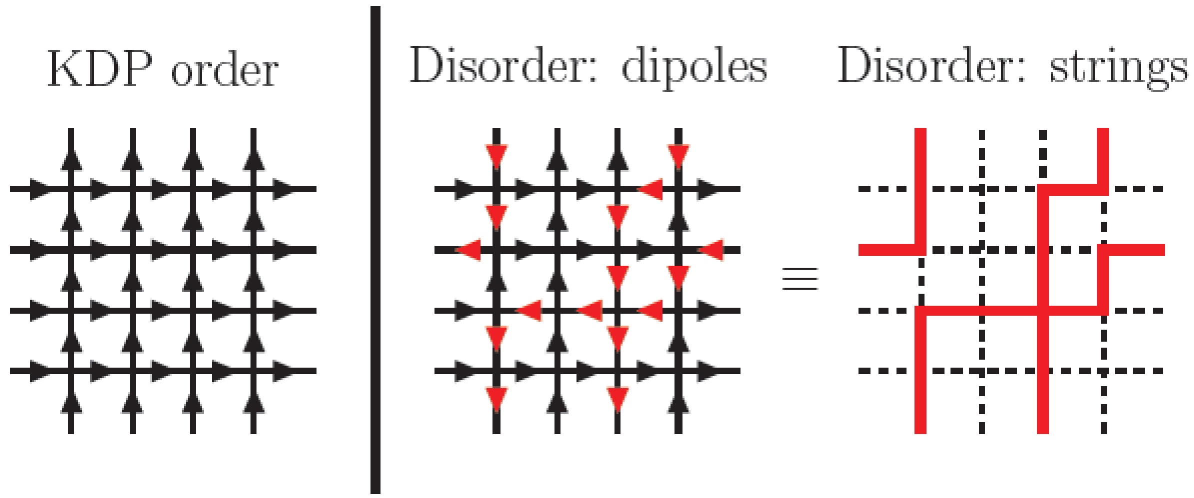

Figure II.10: **Configurations of the 6-vertex model:** *Left:* One of the two ground states of the KDP model with a net polarisation pointing north-east. *Right:* an example of disordered state represented with both dipoles and strings. We impose periodic boundary conditions.

Emergent phenomena

nature Vol 451|3 January 2008|doi:10.1038/nature06433

Magnetic monopoles in spin ice

C. Castelnovo[1], R. Moessner[1,2] & S. L. Sondhi[3]

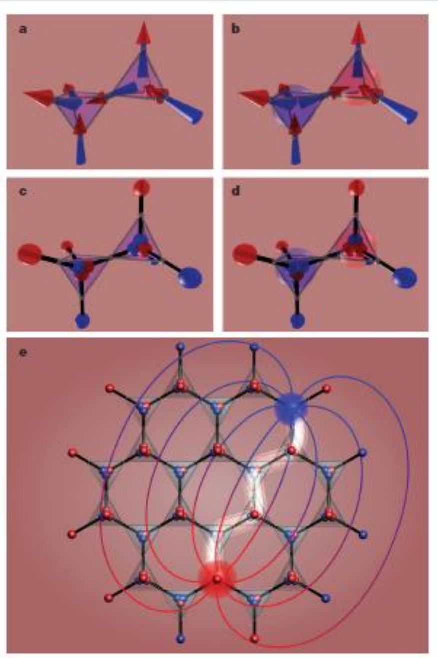

Journal of Experimental and Theoretical Physics, Vol. 101, No. 3, 2005, pp. 481–486.
Translated from Zhurnal Eksperimental'noi i Teoreticheskoi Fiziki, Vol. 128, No. 3, 2005, pp. 559–566.

ORDER, DISORDER, AND PHASE TRANSITIONS IN CONDENSED SYSTEMS

Magnetic Relaxation in Rare-Earth Oxide Pyrochlores

I. A. Ryzhkin

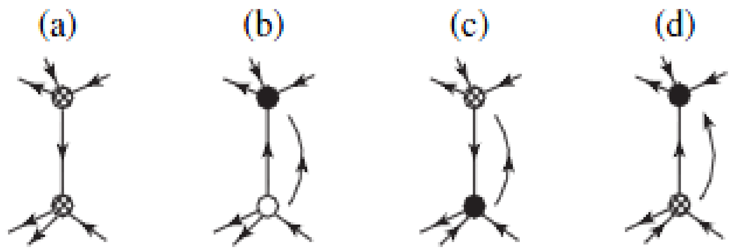

Fig. 3. Fragments of magnetic lattices with (a) no defects, (b) a pair of magnetic defects created by flipping a spin on the vertical bond, and (c, d) displacement of a magnetic defect downwards by a lattice spacing caused by a spin flip on the vertical bond. Hatched, closed, and open circles represent defect-free vertices and positive and negative magnetic defects, respectively.

$$\vec{\nabla}.\vec{S}=0$$

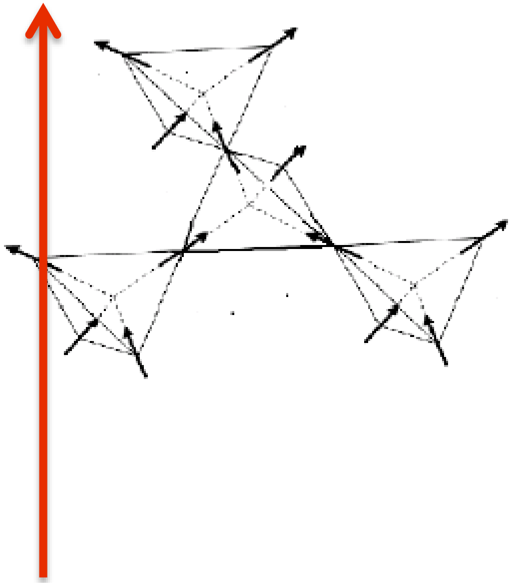

Topological constraints
Excitations back to paramagnet….

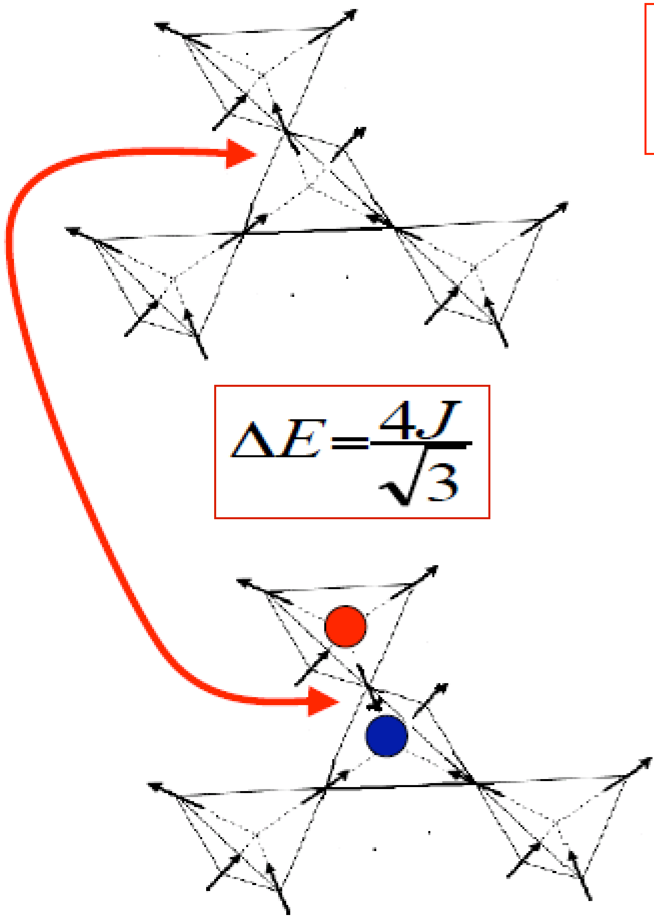

$$\Delta E = \frac{4J}{\sqrt{3}}$$

Topological constraints
3in-1out defects can be created

- 3 out- 1 in
- 3 in 1 out

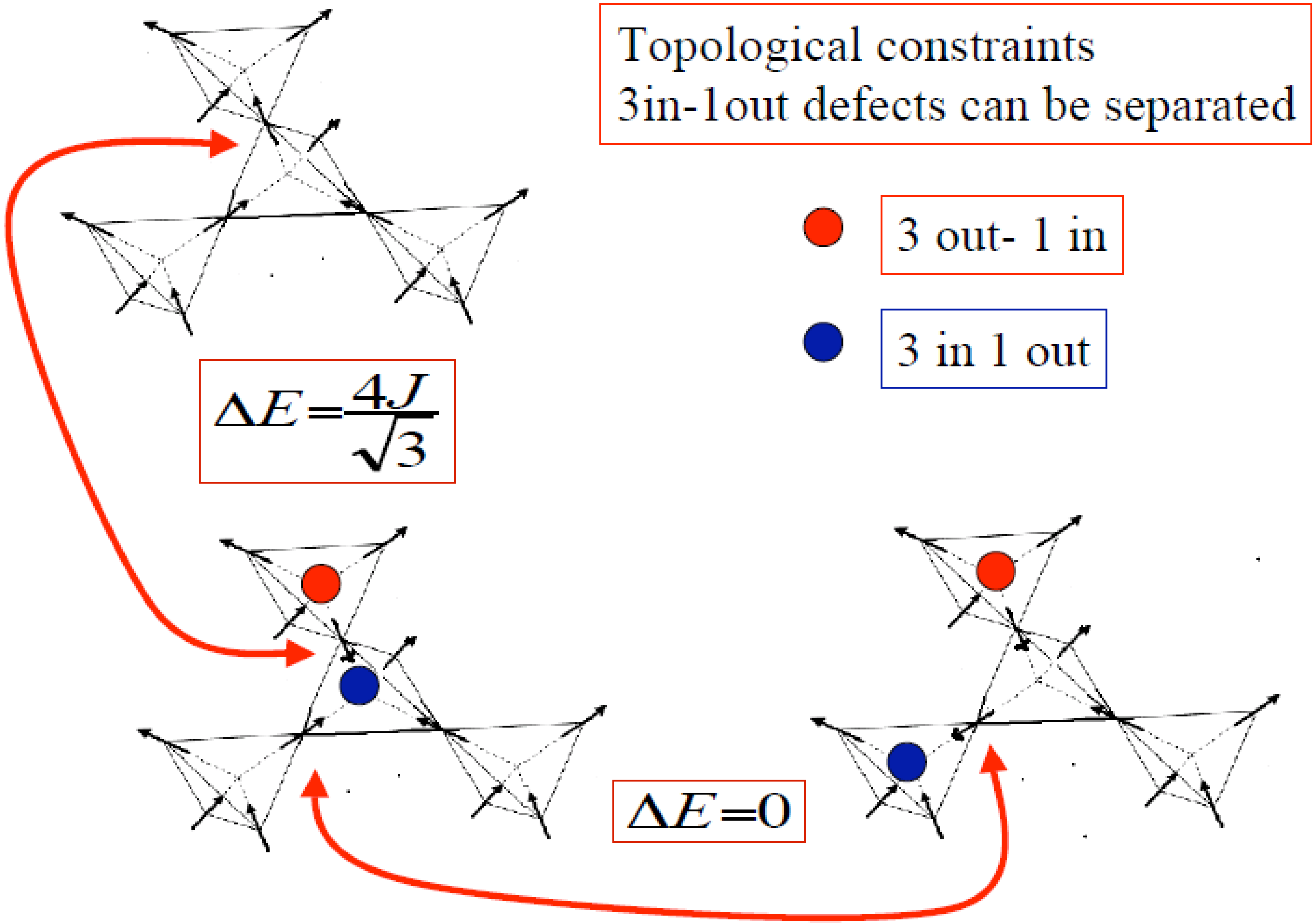

Topological constraints
3in-1out defects can be separated
3 out- 1 in
3 in 1 out
$\Delta E = \frac{4J}{\sqrt{3}}$
$\Delta E = 0$

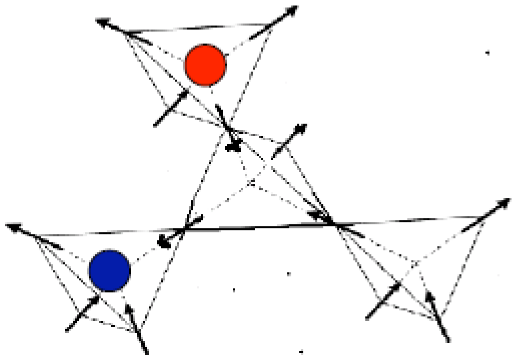

Topological defects (monopoles)
can only be created/destroyed in pairs

Including dipole interactions the defects interact
Castelnovo, Moessner, Sondhi, Nature, 451, 42, 2008

nature Vol 451|3 January 2008|doi:10.1038/nature06433

Magnetic monopoles in spin ice

C. Castelnovo[1], R. Moessner[1,2] & S. L. Sondhi[3]

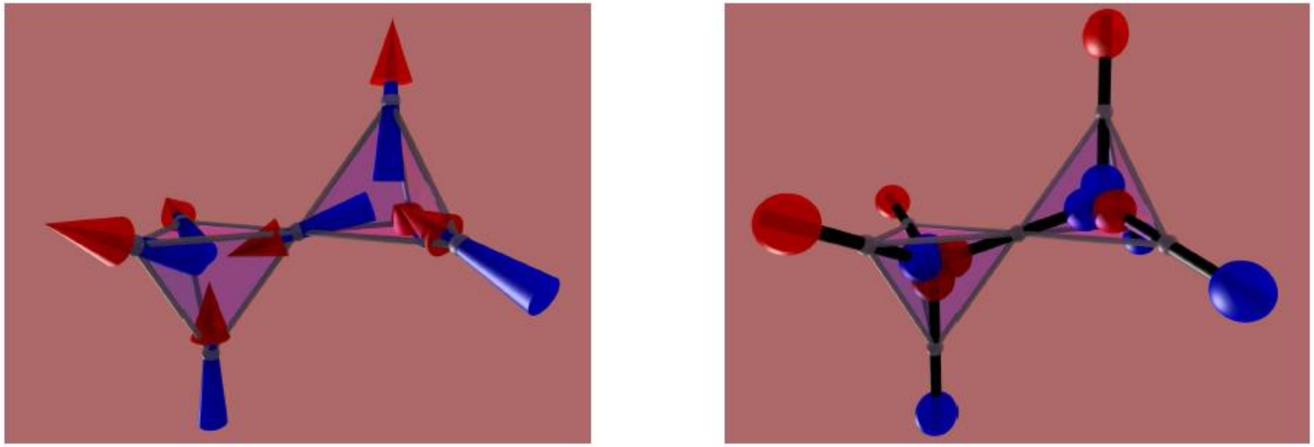

FIG. SI-1: Mapping from dipoles to dumbells. Left: two neighboring tetrahedra obeying the ice rule, with two spins pointing in and two out, giving zero net charge on each site. Right: The corresponding dumbell picture obtained by replacing each spin by a pair of opposite magnetic charges placed on the adjacent sites of the diamond lattice.

Given a configuration of N dipoles, let us label $\{q_i,\ i = 1, \ldots, 2N\}$ the $2N$ charges in the corresponding dumbell configuration. The magnetic Coulomb interaction between the charges is given by

$$\mathcal{V}(r_{ij}) = \begin{cases} \frac{\mu_0}{4\pi}\frac{q_i q_j}{r_{ij}} & r_{ij} \neq 0 \\ v_0 q_i q_j & r_{ij} = 0, \end{cases} \qquad (1.2)$$

nature Vol 451|3 January 2008|doi:10.1038/nature06433

Magnetic monopoles in spin ice

C. Castelnovo[1], R. Moessner[1,2] & S. L. Sondhi[3]

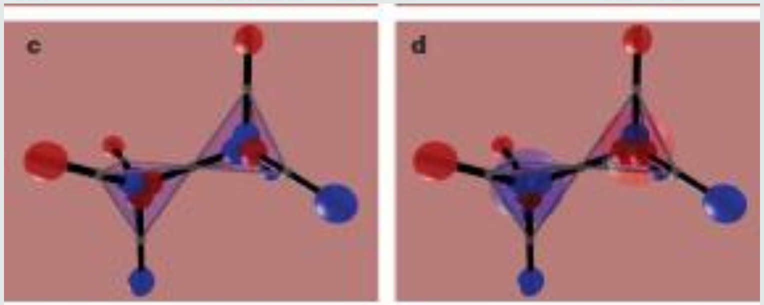

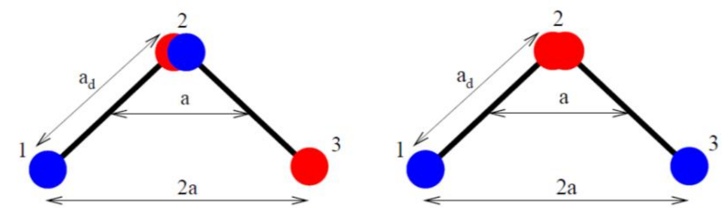

FIG. SI-2: Schematic examples of two neighbouring dipoles on the pyrochlore lattice.

I. THE DUMBELL PICTURE

This material presents a detailed derivation of the dumbell Hamiltonian used extensively in our paper. We start from the generally accepted Hamiltonian which contains a sum of nearest-neighbour exchange and long range dipolar interactions,

$$H = \frac{J}{3}\sum_{\langle ij\rangle} S_i S_j + Da^3 \sum_{(ij)} \left[\frac{\hat{e}_i \cdot \hat{e}_j}{|\mathbf{r}_{ij}|^3} - \frac{3\left(\hat{e}_i \cdot \mathbf{r}_{ij}\right)\left(\hat{e}_j \cdot \mathbf{r}_{ij}\right)}{|\mathbf{r}_{ij}|^5} \right] S_i S_j \tag{1.1}$$

The magnetic moment of a spin is denoted by μ, which equals approximately 10 Bohr magnetons ($\mu = 10\mu_B$) for the spin ice compounds discussed here (namely, $Dy_2Ti_2O_7$ and $Ho_2Ti_2O_7$). The distance between spins is r_{ij}, and $a \simeq 3.54$ Å is the pyrochlore nearest-neighbour distance. $D = \mu_0\mu^2/(4\pi a^3) = 1.41$K is the coupling constant of the dipolar interaction.

A dipole can be thought of as a pair of equal and opposite charges of strength $\pm q$, separated by a distance $\tilde{a}$, such that $\mu = q\tilde{a}$. The dipolar part of the Hamiltonian is reproduced exactly in the limit $\tilde{a} \to 0$. Here we choose $\tilde{a}$ to equal the diamond lattice constant $a_d = \sqrt{3/2}\, a$, therefore fixing $q = \mu/a_d$. The two ways of assigning charges reproduce the two orientations of the original dipole, as illustrated in Fig. SI-1

nature Vol 451|3 January 2008|doi:10.1038/nature06433

Magnetic monopoles in spin ice

C. Castelnovo[1], R. Moessner[1,2] & S. L. Sondhi[3]

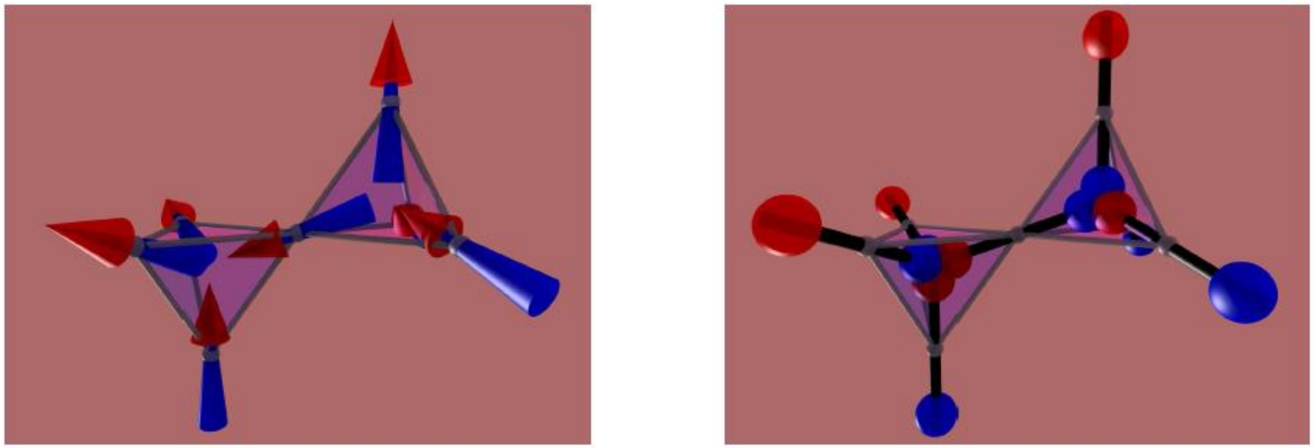

FIG. SI-1: Mapping from dipoles to dumbells. Left: two neighboring tetrahedra obeying the ice rule, with two spins pointing in and two out, giving zero net charge on each site. Right: The corresponding dumbell picture obtained by replacing each spin by a pair of opposite magnetic charges placed on the adjacent sites of the diamond lattice.

Given a configuration of N dipoles, let us label $\{q_i,\ i = 1,\ \ldots,\ 2N\}$ the $2N$ charges in the corresponding dumbell configuration. The magnetic Coulomb interaction between the charges is given by

$$\mathcal{V}(r_{ij}) = \begin{cases} \frac{\mu_0}{4\pi}\frac{q_i q_j}{r_{ij}} & r_{ij} \neq 0 \\ v_0 q_i q_j & r_{ij} = 0, \end{cases} \qquad (1.2)$$

nature Vol 451|3 January 2008|doi:10.1038/nature06433

Magnetic monopoles in spin ice

C. Castelnovo[1], R. Moessner[1,2] & S. L. Sondhi[3]

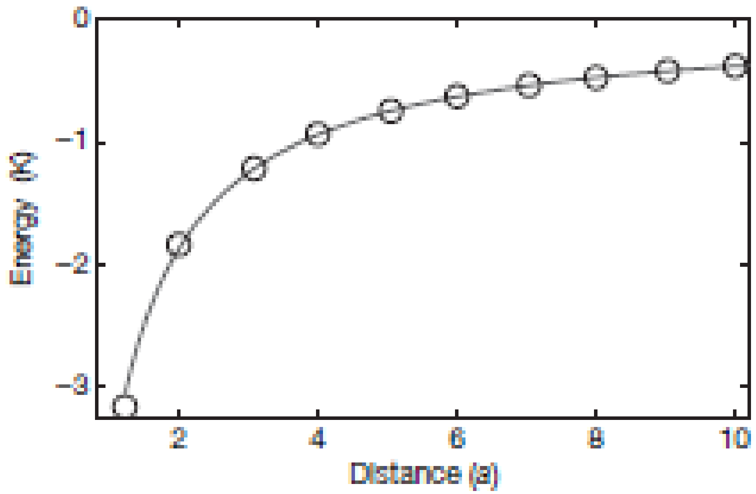

Figure 3 | Monopole interaction. Comparison of the magnetic Coulomb energy $-\mu_0 q_m^2/(4\pi r)$ (equation (2); solid line) with a direct numerical evaluation of the monopole interaction energy in dipolar spin ice (equation (1); open circles), for a given spin-ice configuration (Fig. 2e), as a function of monopole separation.

Measurement of the charge and current of magnetic monopoles in spin ice

S. T. Bramwell[1]*, S. R. Giblin[2]*, S. Calder[1], R. Aldus[1], D. Prabhakaran[3] & T. Fennell[4]

an example being the autoionization of water or water ice:

$$2H_2O = [H_3O^+ OH^-] = H_3O^+ + OH^-$$

Onsage ... nsional
Coulombi ... ria:

quasipar ... es (1)

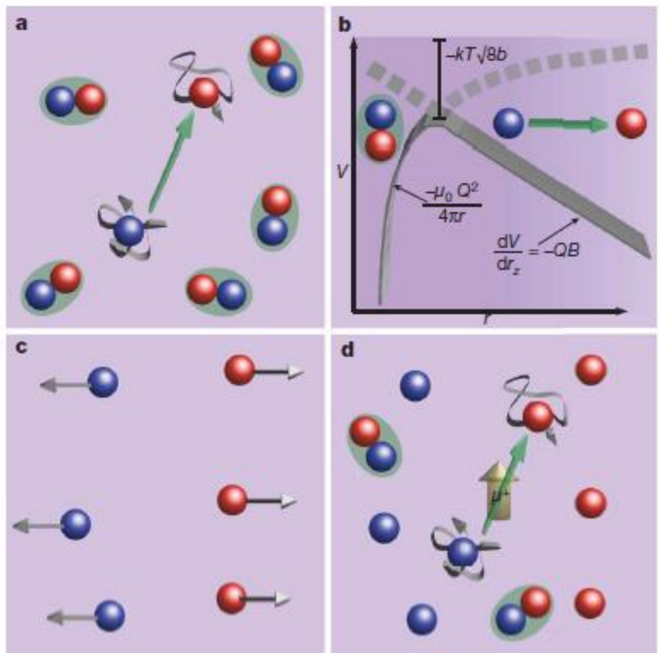

Figure 1 | Magnetic Wien effect, and the detection of magnetic charge by implanted muons. **a**, In zero field, magnetic charges occur as bound pairs, but some dissociate to give a fluctuating magnetic moment (green arrow). **b**, The field energy $-QBr_z$ competes with the Coulomb potential $-\mu_0 Q^2/4\pi r$ to lower the activation barrier to dissociation. **c**, The application of a transverse field causes dissociation as charges are accelerated by the field. **d**, In the applied field, these charges remain dissociated while more bound pairs form to restore equilibrium. Magnetic moment fluctuations due to free charges produce local fields that are detected by implanted muons (μ^+).

$$K = n_0 \frac{\alpha^2}{1-\alpha} \qquad (5)$$

VIP Neutron DIFFRACTOMETER (5C1) LLB

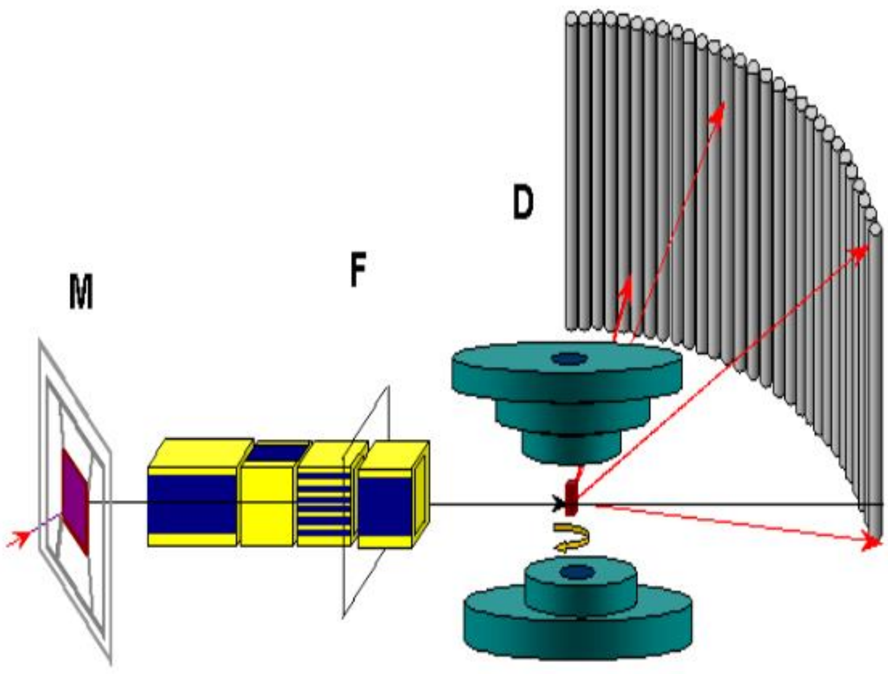

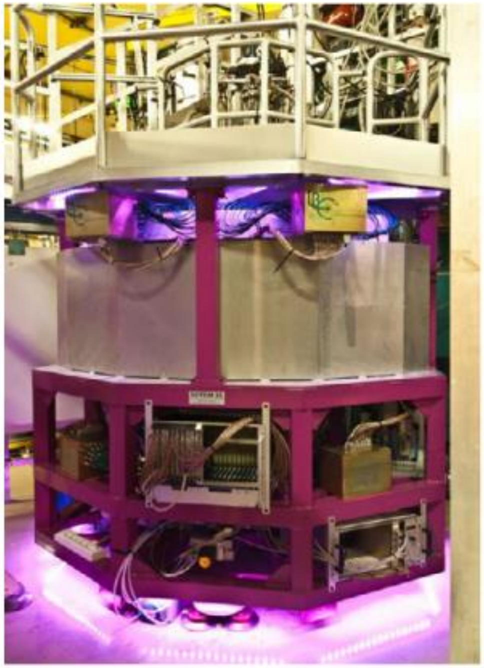

80°x25°, λ=0.84 Å

VIP Neutron DIFFRACTOMETER (5C1) LLB

Yb2Ti207   2 K, 1T
V~60mm3

3500 steps of 0.1°
Exposition 4 sec/frame

951 reflections observed

526   (R-1)> 3σ

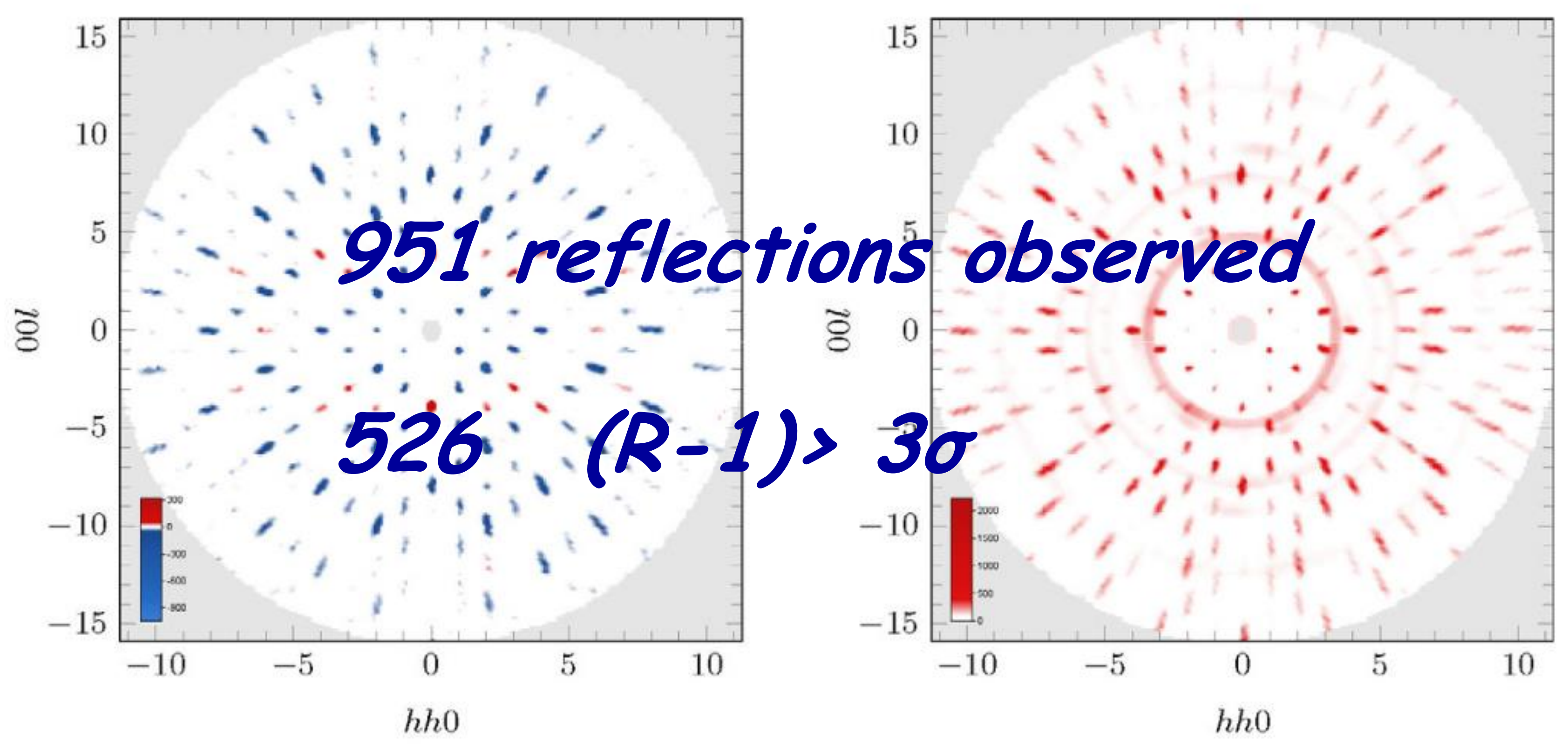

Fig. 3. Two dimensional cuts in the reciprocal space measured on VIP from $Yb_2Ti_2O_7$ (about 100 mm^3) during 5 hours. Left panel: The difference $I^+ - I^-$. Right panel: The sum $I^+ + I^-$.

PRL 103, 056402 (2009) PHYSICAL REVIEW LETTERS week ending 31 JULY 2009

Ising versus *XY* Anisotropy in Frustrated $R_2Ti_2O_7$ Compounds as "Seen" by Polarized Neutrons

H. Cao,[1] A. Gukasov,[1] I. Mirebeau,[1] P. Bonville,[2] C. Decorse,[3] and G. Dhalenne[3]

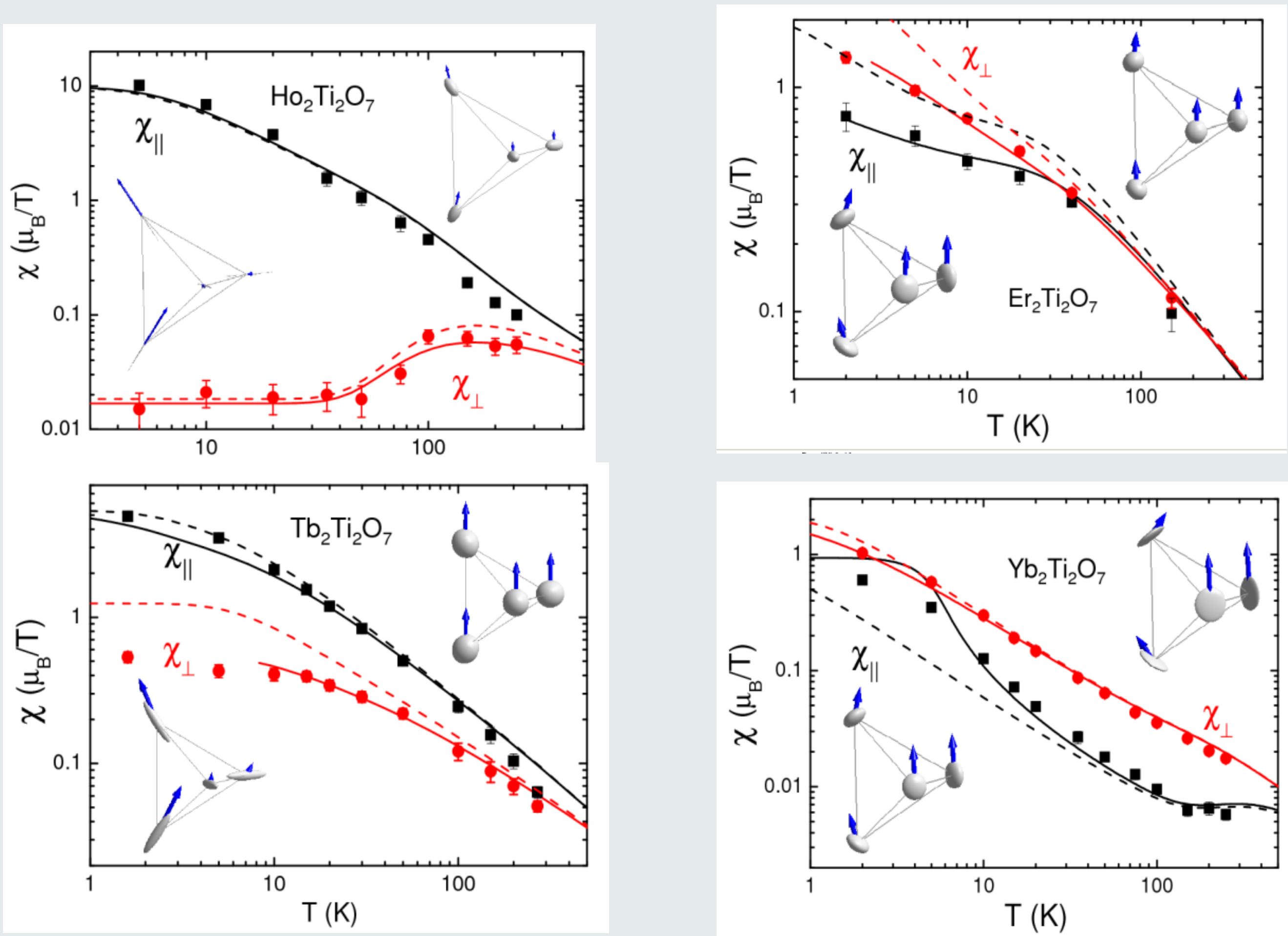

Spin Ice under Magnetic Field

VOLUME 81, NUMBER 20 PHYSICAL REVIEW LETTERS 16 NOVEMBER 1998

Liquid-Gas Critical Behavior in a Frustrated Pyrochlore Ferromagnet

M. J. Harris,[1] S. T. Bramwell,[2] P. C. W. Holdsworth,[3] and J. D. M. Champion[1,2,3]

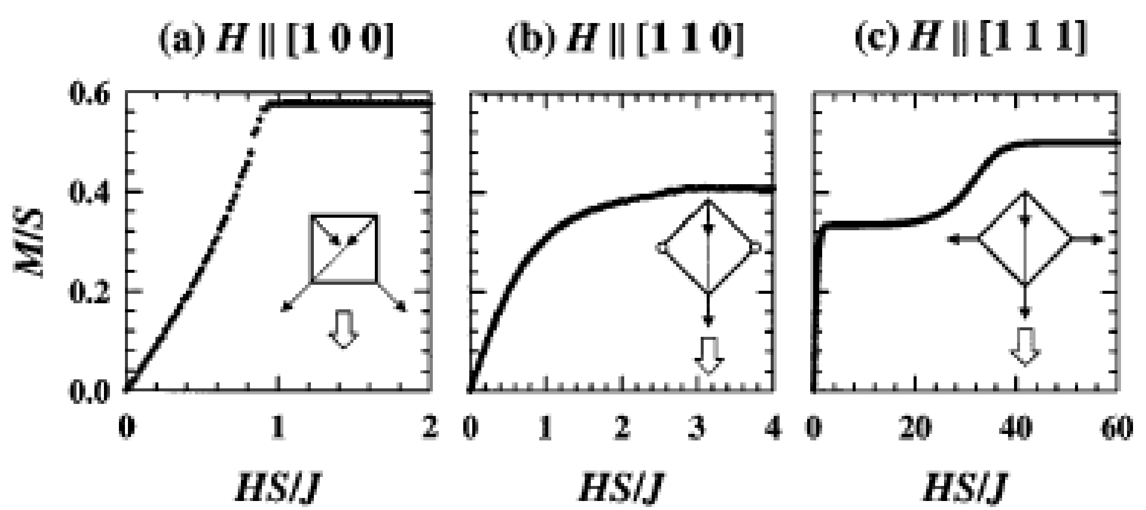

Journal of the Physical Society of Japan
Vol. 78, No. 10, October, 2009, 103706

Observation of Magnetic Monopoles in Spin Ice

Hiroaki KADOWAKI[1], Naohiro DOI[1], Yuji AOKI[1], Yoshikazu TABATA[2],
Taku J. SATO[3], Jeffrey W. LYNN[4],
Kazuyuki MATSUHIRA[5], and Zenji HIROI[6]

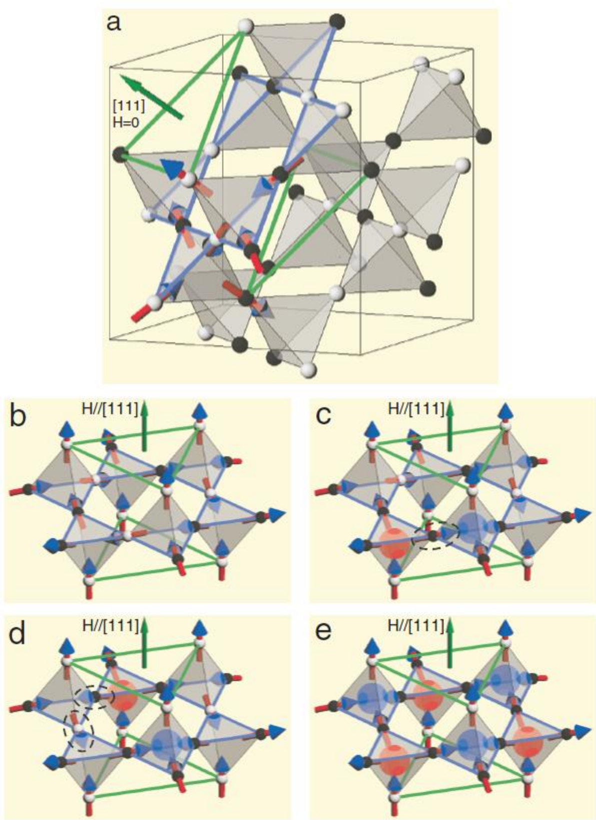

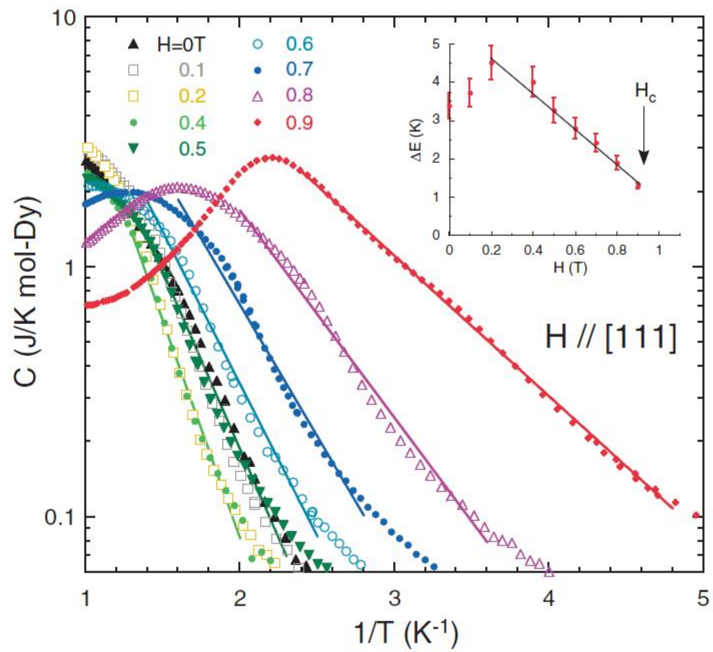

Fig. 2. Specific heat under [111] fields is plotted as a function of $1/T$. In the intermediate temperature range these data are well represented by the Arrhenius law denoted by solid lines. The inset shows the field dependence of the activation energy.

Double-layered monopolar order in $Tb_2Ti_2O_7$ spin liquid

A. P. Sazonov,* A. Gukasov, and I. Mirebeau
CEA, Centre de Saclay, DSM/IRAMIS/Laboratoire Léon Brillouin, F-91191 Gif-sur-Yvette, France

P. Bonville
CEA, Centre de Saclay, DSM/IRAMIS/Service de Physique de l'Etat Condensé, F-91191 Gif-Sur-Yvette, France
(Dated: February 23, 2012)

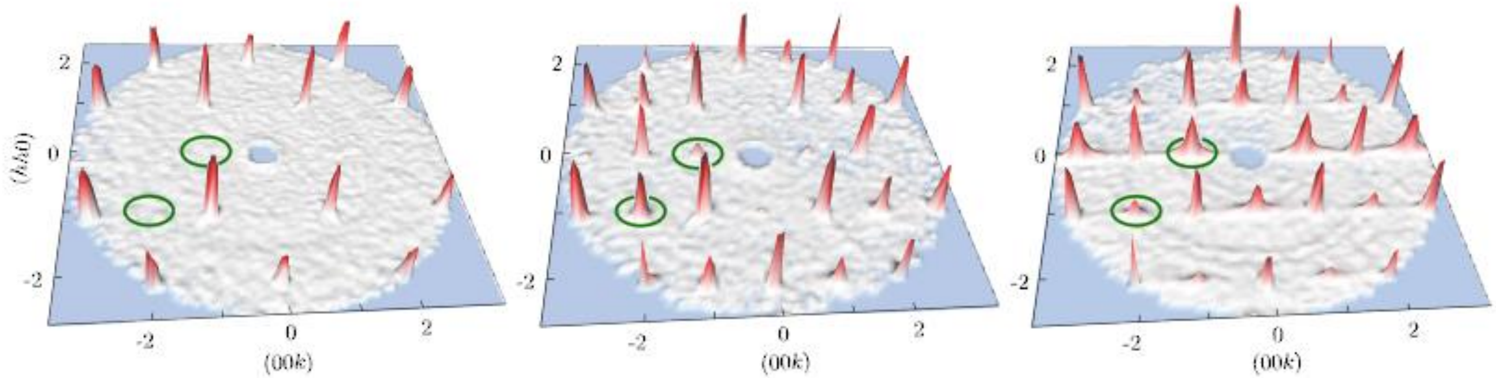

FIG. 2. Neutron scattering of $Tb_2Ti_2O_7$ in 0 T (left panel), $Tb_2Ti_2O_7$ in 5 T (middle panel) and $Ho_2Ti_2O_7$ in 2 T (right panel) at 1.6 K with $\boldsymbol{H} \parallel [110]$. Intensity is given in a logarithmic scale. Selected magnetic reflections are highlighted. In zero field, only the peaks of the crystal structure are seen.

Table 2. Irreducible representations Γ'_3 and Γ'_2 of $R_2Ti_2O_7$ (space group $I4_1/amd$) associated with $\boldsymbol{k} = (0,0,1)$. Basis vectors projected from a general vector $\boldsymbol{M}$ with components M_x, M_y, M_z at the the R 8d sites. The Tb positions are defined in Table 1.

Irr. rep.	Atom	M_x	M_y	M_z
Γ'_3	R-α_1	0	U'_y	U'_z
	R-α_2	0	U'_y	$-U'_z$
	R-β_1	V'_x	0	$-V'_z$
	R-β_2	V'_x	0	V'_z
Γ'_2	R-α_1	0	$U'+V'$	$U'_z+V'_z$
	R-α_2	0	$-U'-V'$	$U'_z+V'_z$
	R-β_1	$U'-V'$	0	$-U'_z+V'_z$
	R-β_2	$-U'+V'$	0	$-U'_z+V'_z$

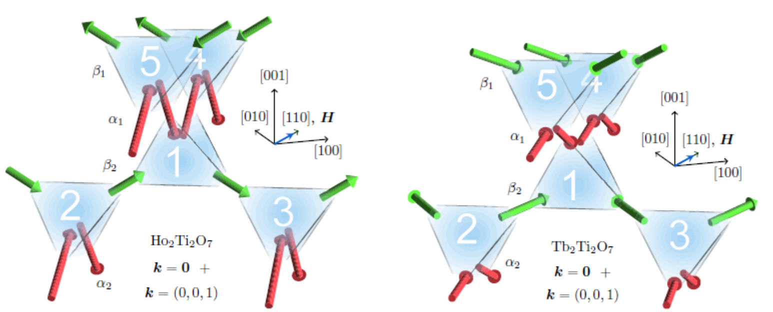

Figure 2. Resulting field-induced magnetic structures of $Ho_2Ti_2O_7$ (left) and $Tb_2Ti_2O_7$ (right, Ref. [8]) calculated as a superposition of the $\boldsymbol{k} = \boldsymbol{0}$ and $\boldsymbol{k} = (0,0,1)$ structures measured at $T = 1.6$ K and $H = 7$ T. Tetrahedra are numbered for an easy comparison with Fig. 1.

Double layered monopole structure in spin liquide

A Sazonov, A Gukasov, I Mirebeau and P Bonville.

Phys. Rev. B **85**, 214420 (2012)

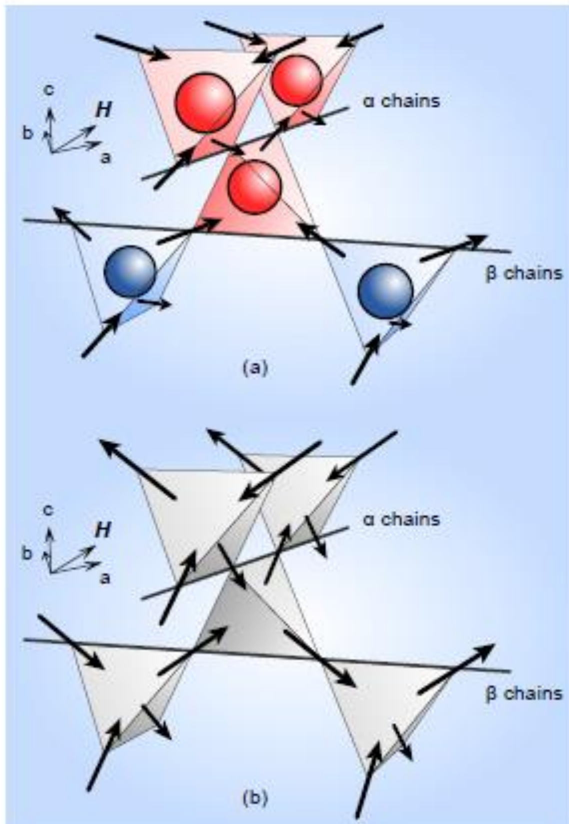

FIG. 3. Magnetic structures of $Tb_2Ti_2O_7$ spin liquid and $Ho_2Ti_2O_7$ spin ice in a [110] field. (a) Antimonopolar (double-layered monopolar) structure of $Tb_2Ti_2O_7$. (b) Magnetically vacuum state of $Ho_2Ti_2O_7$.

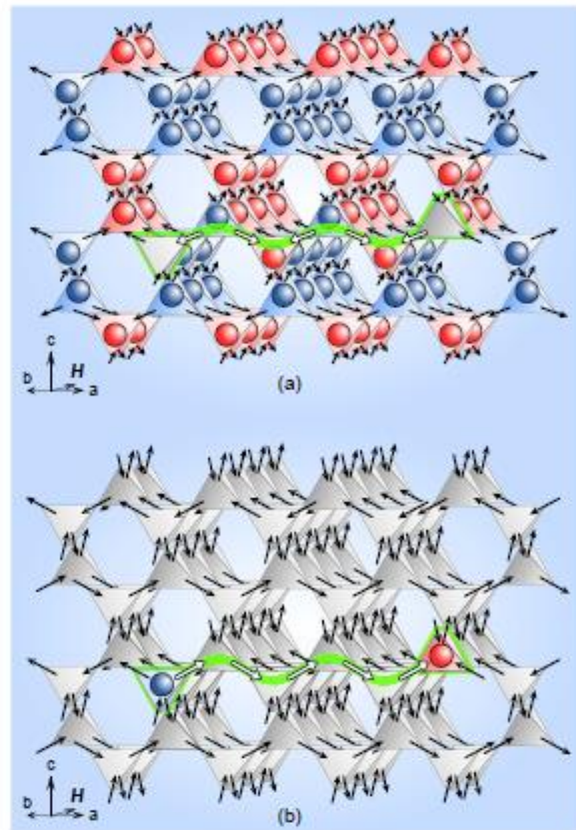

FIG. 4. Elementary excitations in $Tb_2Ti_2O_7$ spin liquid and $Ho_2Ti_2O_7$ spin ice. (a) Antimonopolar (double-layered monopolar) structure of $Tb_2Ti_2O_7$ with vacuum pair excitations. (b) Magnetically vacuum state of $Ho_2Ti_2O_7$ with

Double layered monopole structure and structural distortions.

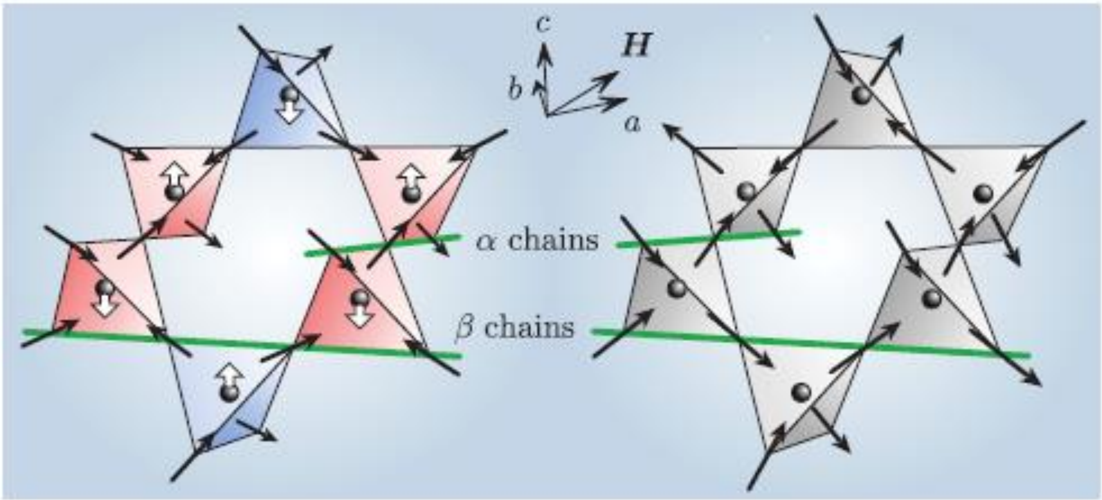

FIG. 6. (Color online) Left panel: The structural distortion in $Tb_2Ti_2O_7$ compatible with the observed high-field magnetic structure. The directions of displacements of the axial oxygens are shown by white arrows. Right panel: The undistorted structure of $Ho_2Ti_2O_7$.

CEF+ Anistropic exchange+Tetragonal Distortion

$$\mathcal{H}_Q = D_Q J_Z^2, \quad (1)$$

which writes in the local frame with [111] as z axis,

$$\mathcal{H}_Q = \frac{D_Q}{3}\left[2J_x^2 + J_z^2 + \sqrt{2}(J_x J_z + J_z J_x)\right]. \quad (2)$$

Quadrupolar Interaction

$$\mathcal{H}_Q = \frac{D_Q}{3}\left[2Q_{xx} + Q_{zz} + \frac{J(J+1)}{3} + 2\sqrt{2}Q_{xz}\right]. \quad (3)$$

$$Q_{xz} = \tfrac{1}{2}(J_x J_z + J_z J_x).$$

Jahn-Teller

$$\mathcal{H}_{JT} = -g_Q \langle Q_{xz} \rangle Q_{xz},$$

PHYSICAL REVIEW B **91**, 214422 (2015)

Multiferroicity in spin ice: Towards magnetic crystallography of $Tb_2Ti_2O_7$ in a field

L. D. C. Jaubert[1] and R. Moessner[2]

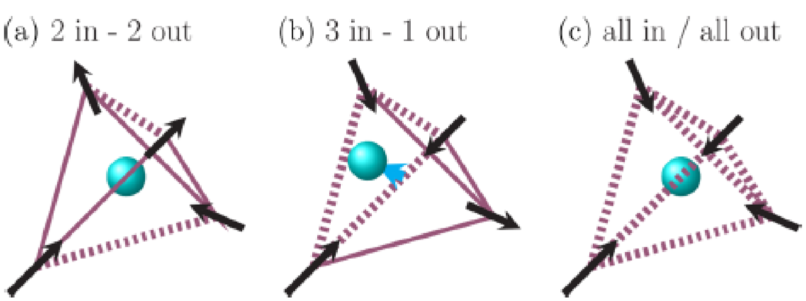

FIG. 2. (Color online) The lowering of the tetrahedral symmetry imposed by the (a) 2 in - 2 out, (b) 3 in - 1 out, and (c) 4 in spin configurations allows for a displacement of the oxygen ion (cyan sphere), and thus an electric polarization, only for the singly charged configurations (b) [21]. The spin configurations of the solid (dashed) bonds are (anti)ferromagnetic.

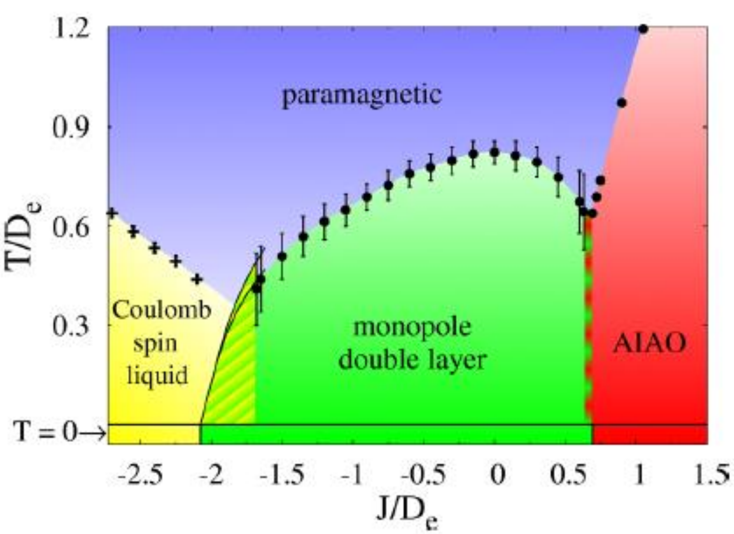

Interestingly, this outcome can also be understood from the spin-current model [3] applied to spin ice [22] where a pair of canted spins can produce an electric dipole of the form

$$\vec{P} \propto \vec{e}_{ij} \times (\vec{S}_i \times \vec{S}_j). \quad (1)$$

Simple arithmetic provides a finite electric moment for singly charged monopoles only.

II. MODEL AND METHODS

We consider the following Hamiltonian:

$$\mathcal{H} = J \sum_{\langle ij \rangle} \vec{S}_i \cdot \vec{S}_j - \vec{h} \cdot \sum_i \vec{S}_i + D_m r_m^3 \sum_{i>j} \frac{\vec{S}_i \cdot \vec{S}_j - 3(\vec{S}_i \cdot \vec{e}_{ij})(\vec{S}_j \cdot \vec{e}_{ij})}{r_{ij}^3} + D_e r_e^3 \sum_{\alpha>\beta} \frac{\vec{P}_\alpha \cdot \vec{P}_\beta - 3(\vec{P}_\alpha \cdot \vec{e}_{\alpha\beta})(\vec{P}_\beta \cdot \vec{e}_{\alpha\beta})}{r_{\alpha\beta}^3}, \quad (2)$$

Double layered *magnetoelectric* monopole structure and structural distortions.

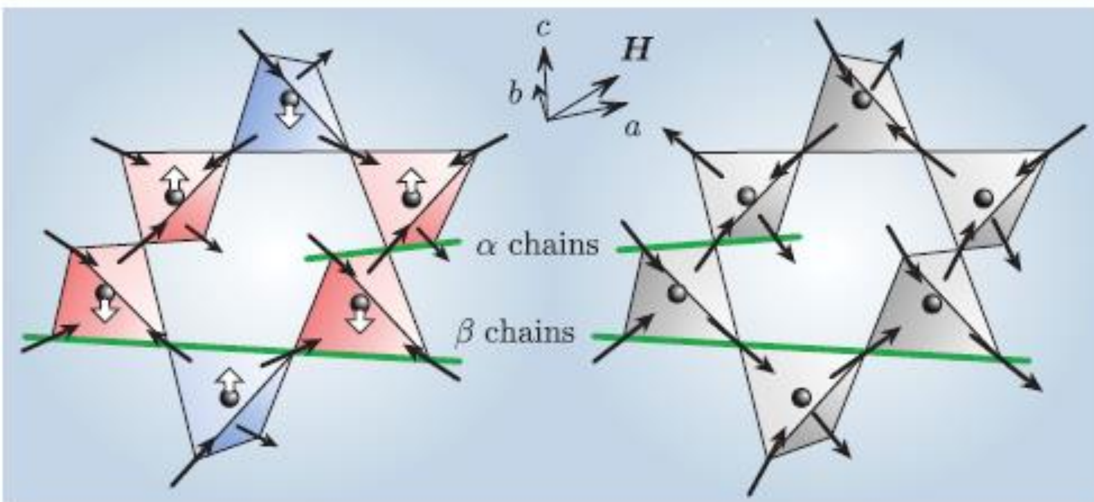

FIG. 6. (Color online) Left panel: The structural distortion in $Tb_2Ti_2O_7$ compatible with the observed high-field magnetic
The directions of displacements of the axial oxygens are
white arrows. Right panel: The undistorted structure of Hc

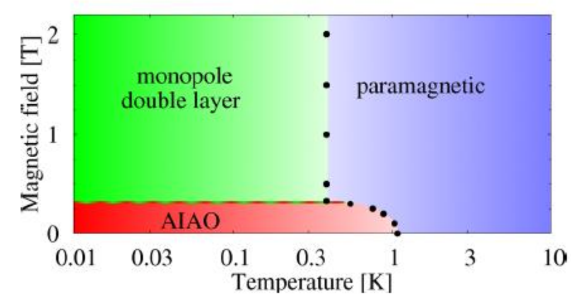

FIG. 6. (Color online) Phase diagram parametrized for $Tb_2Ti_2O_7$ for $J = 2.7$ K, $D_m = 0.48$ K, and $D_e = 0.32$ K. The [110] magnetic field aligns the α chains along the [110] direction, destroying the AIAO order in favor of the double-layer structure. All error bars are smaller than the dots except for the red/green hatched region where simulations were difficult to equilibrate.

Conclusions

L. D. C. JAUBERT AND R. MOESSNER. Phys. Rev. B91 214422 (2015)

- magnetoelectric coupling can lift the degeneracy of a spin ice by creating interactions between topological excitations. These excitations condense into a bilayered monopole crystal, a nontrivial example of “magnetic crystallography.”

- New additional, ferroic, degree of freedom will bring a newflavor to spin ice and spin liquids, both at equilibrium and dynamically

Journal of the Physical Society of Japan
Vol. 78, No. 10, October, 2009, 103706

LETTERS

Observation of Magnetic Monopoles in Spin Ice

Hiroaki KADOWAKI[1], Naohiro DOI[1], Yuji AOKI[1], Yoshikazu TABATA[2],
Taku J. SATO[3], Jeffrey W. LYNN[4],
Kazuyuki MATSUHIRA[5], and Zenji HIROI[6]

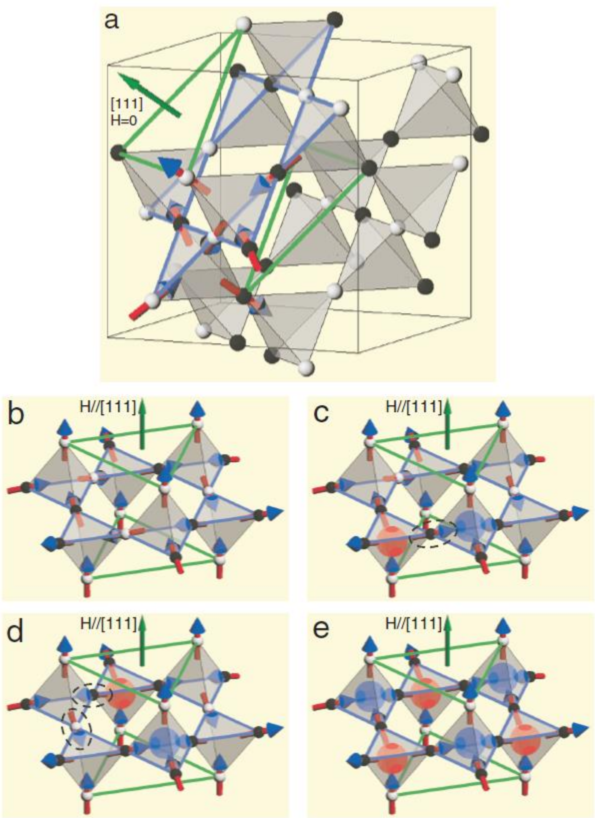

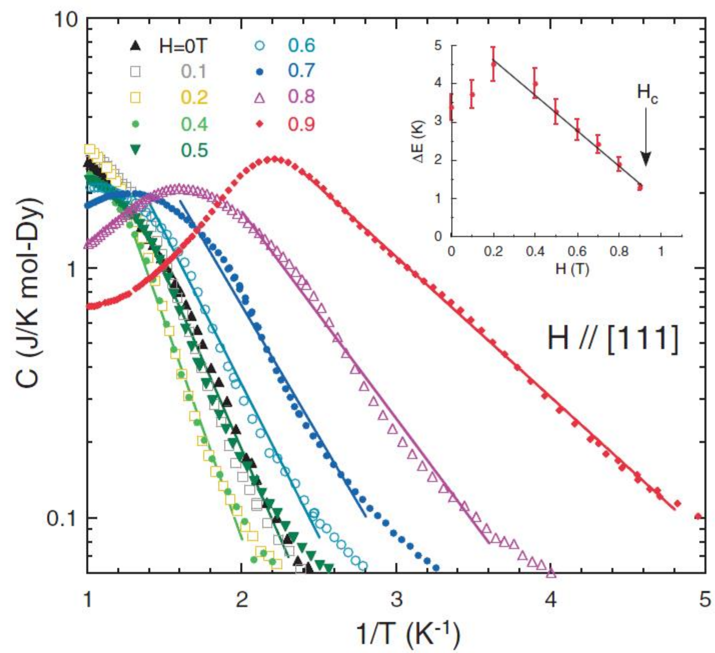

Fig. 2. Specific heat under [111] fields is plotted as a function of $1/T$. In the intermediate temperature range these data are well represented by the Arrhenius law denoted by solid lines. The inset shows the field dependence of the activation energy.

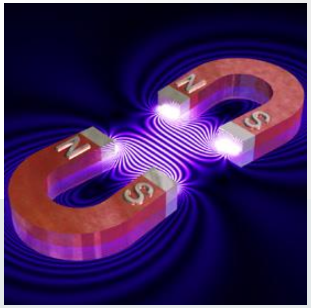

Magnetic ordering

- Ferror

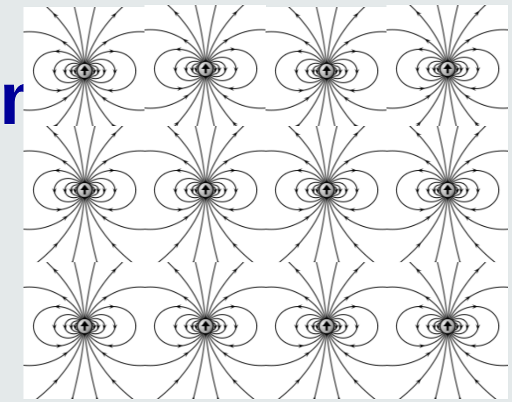

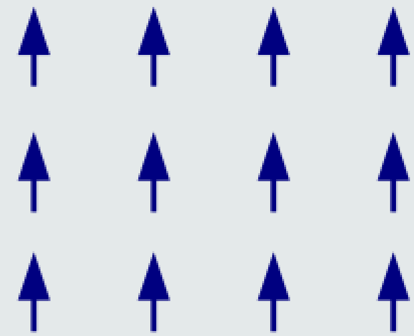

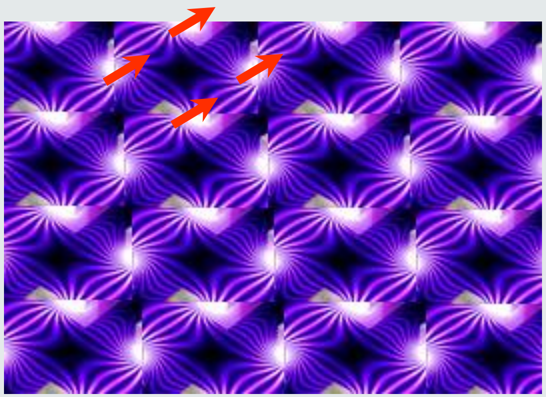

- Antiferromagnetic

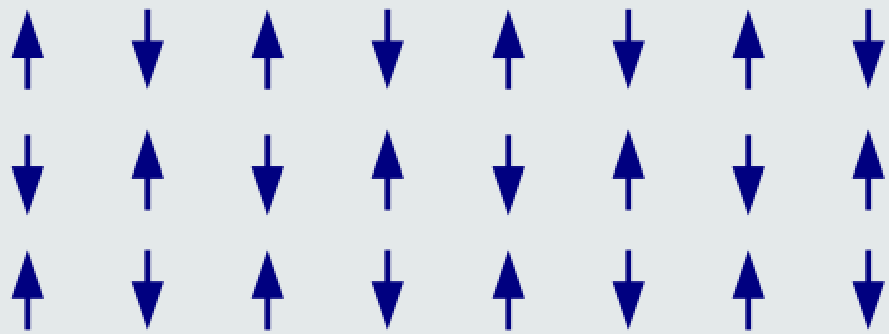

Monopole deconfinement in 2D (NxN size)

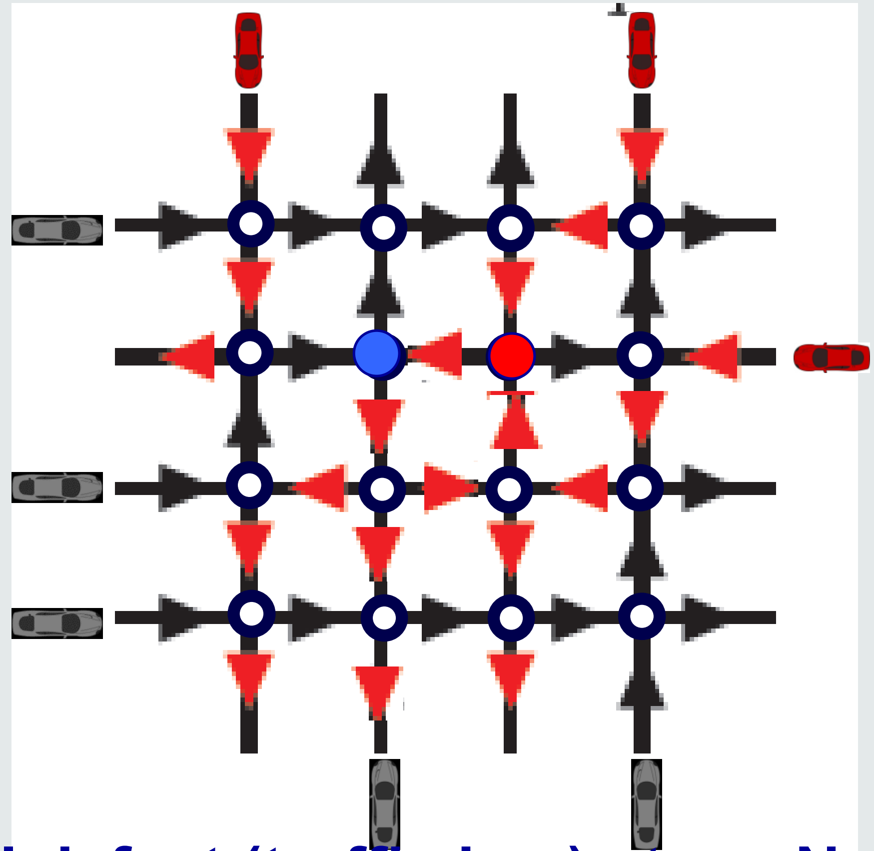

Topological defect (traffic jam) stops N cars but don’t interrupt traffic of majority of them (NxN-N)

Monopole deconfinement in 2D

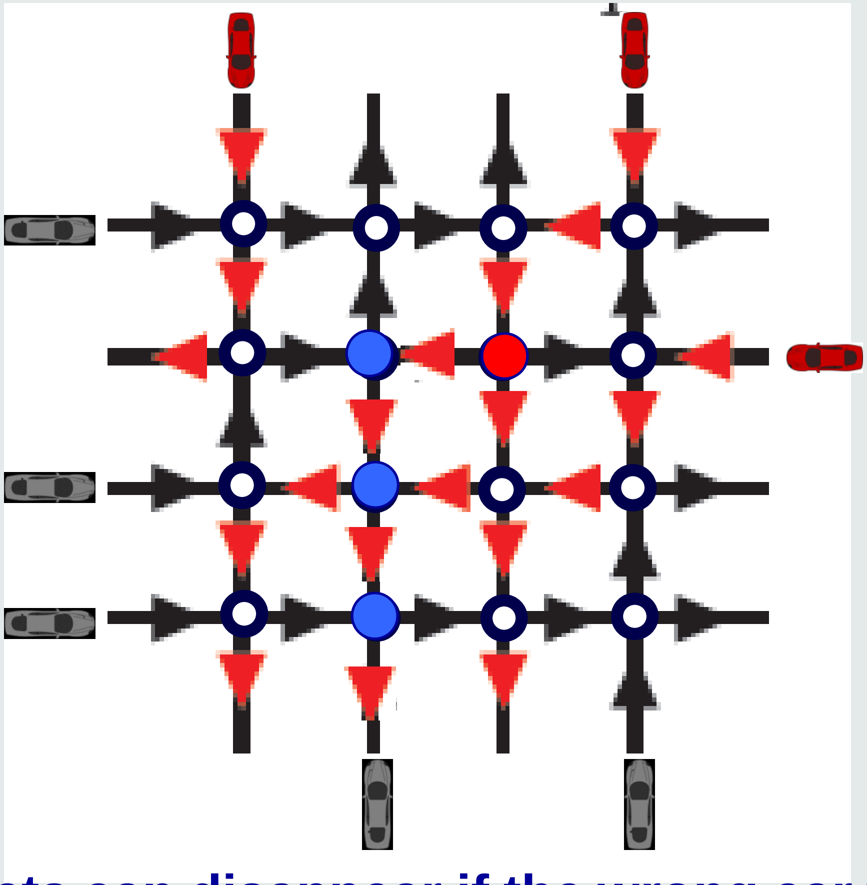

Topological defects can disappear if the wrong car will manage to leave the city or make closed loops due to the speed fluctuations;

Dipolar Interactions and Origin of Spin Ice in Ising Pyrochlore Magnets

Byron C. den Hertog[1] and Michel J. P. Gingras[1,2]

Our Hamiltonian describing the Ising pyrochlore magnets is as follows:

$$H = -J \sum_{\langle ij \rangle} \mathbf{S}_i^{z_i} \cdot \mathbf{S}_j^{z_j} + D r_{\mathrm{nn}}^3 \sum_{j>i} \frac{\mathbf{S}_i^{z_i} \cdot \mathbf{S}_j^{z_j}}{|\mathbf{r}_{ij}|^3} - \frac{3(\mathbf{S}_i^{z_i} \cdot \mathbf{r}_{ij})(\mathbf{S}_j^{z_j} \cdot \mathbf{r}_{ij})}{|\mathbf{r}_{ij}|^5}, \quad (1)$$

where the spin vector $\mathbf{S}_i^{z_i}$ labels the Ising moment of magnitude $|S| = 1$ at lattice site i and *local* Ising axis z_i. Because the local Ising axes belong to the set of $\langle 111 \rangle$ vectors, the nearest-neighbor exchange energy between two spins i and j is $J_{\mathrm{nn}} \equiv J/3$. The dipole-dipole interaction at nearest neighbor is $D_{\mathrm{nn}} \equiv 5D/3$ where D is the usual estimate of the dipole energy scale, $D = (\mu_0/4\pi)g^2\mu^2/r_{\mathrm{nn}}^3$. For both $Ho_2Ti_2O_7$ and $Dy_2Ti_2O_7$, $D_{\mathrm{nn}} \sim 2.35$ K.

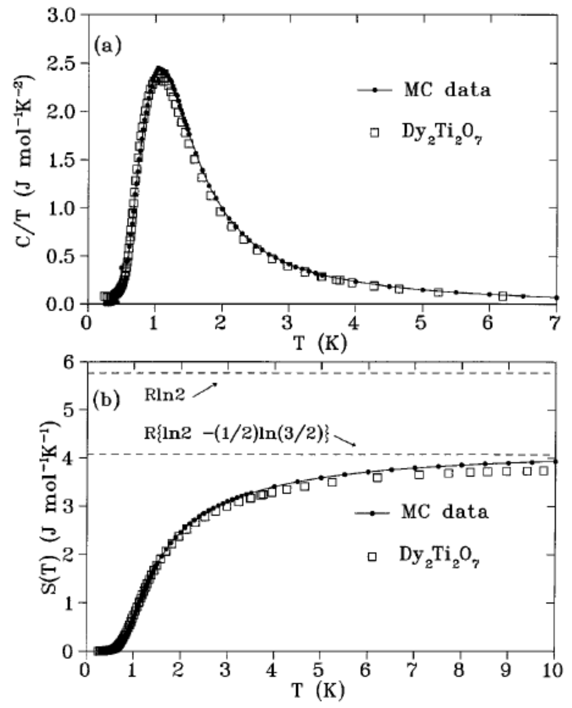

FIG. 3. Comparison of (a) specific heat and (b) entropy data between $Dy_2Ti_2O_7$ [2] and Monte Carlo simulation with $J_{nn} = -1.24$ K, $D_{nn} = 2.35$ K, and system size $L = 4$.

Dipolar Spin Ice (DSI)

Magnetic « Giauque and Stout » experiment:

Ramirez et al, Nature399,333, (1999)

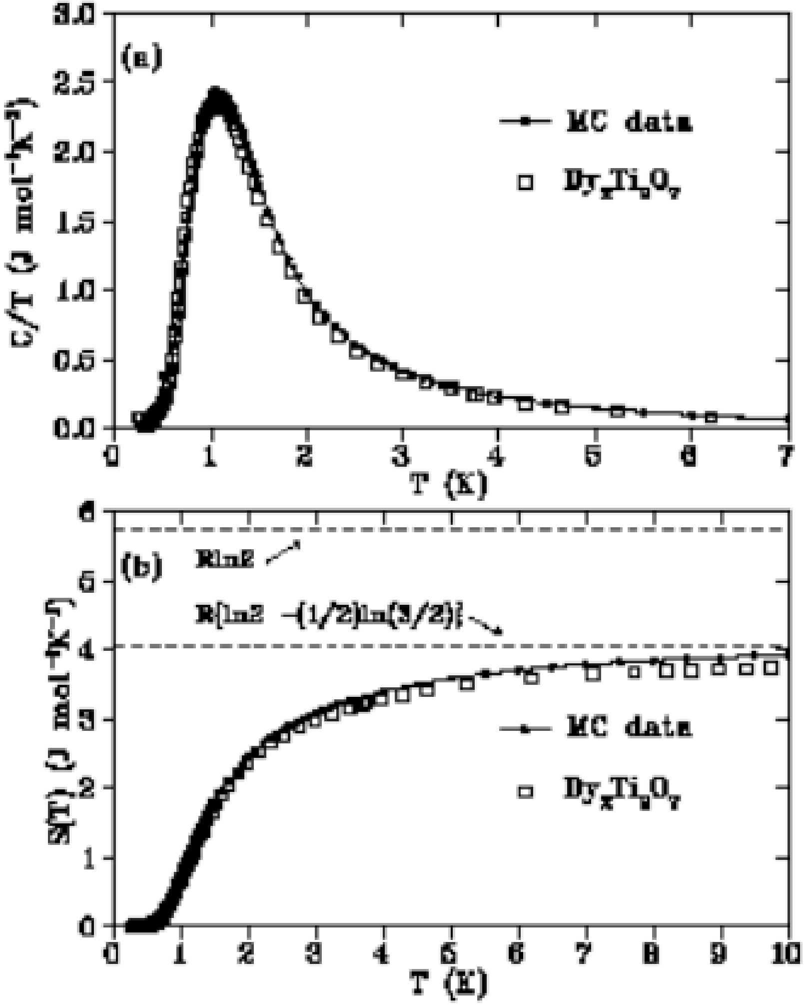

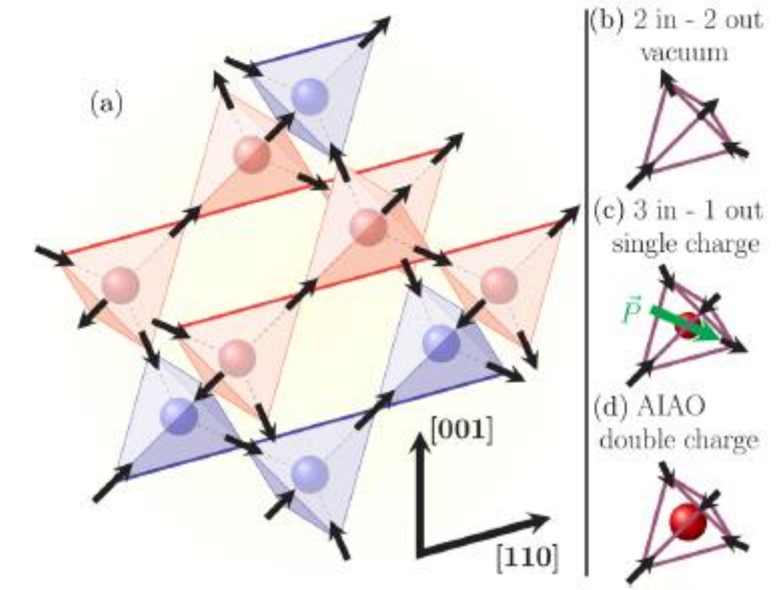

FIG. 1. (Color online) (a) Electrically induced ground state of our multiferroic spin ice model, made of alternative bilayers of positive (blue) and negative (red) magnetic charges stacked along a [001] axis. The α chains (indicated by thick bonds) carry a

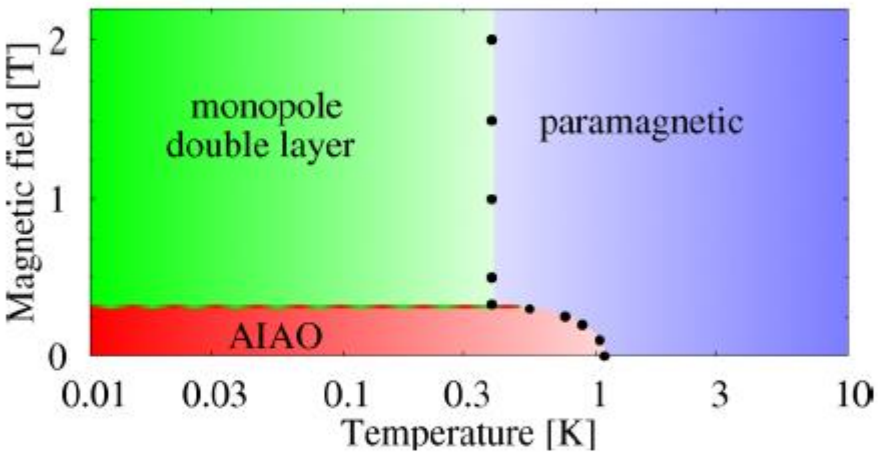

FIG. 6. (Color online) Phase diagram parametrized for $Tb_2Ti_2O_7$ for $J = 2.7$ K, $D_m = 0.48$ K, and $D_e = 0.32$ K. The [110] magnetic field aligns the α chains along the [110] direction, destroying the AIAO order in favor of the double-layer structure. All error bars are smaller than the dots except for the red/green hatched region where simulations were difficult to equilibrate.

Residual entropy of Ice. Pauling entropy

Residual entropy is the difference in entropy between disordered and ordered state at absolute zero.

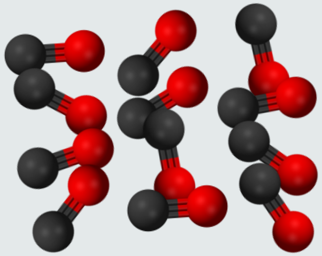

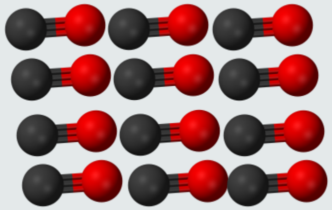

S=Rln(2)

S=0